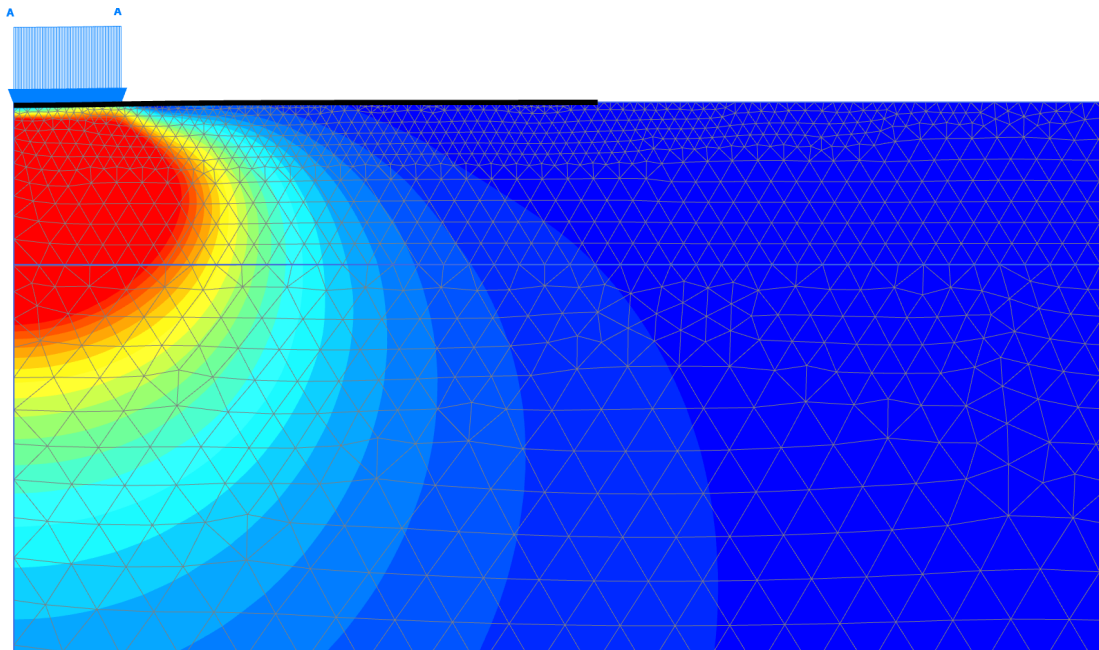


# CHALMERS



## Evaluation of plastic mats as access roads to wind farms

A study of how plastic mats deform and distribute stress on different soils

*Master of Science Thesis in the Master's Programme Industrial Ecology*

VICTOR GILLHOLM & ISAC ROSANDER

Department of Civil and Environmental Engineering  
Division of GeoEngineering  
Road and Traffic Research Group  
CHALMERS UNIVERSITY OF TECHNOLOGY  
Göteborg, Sweden 2014  
Master's Thesis 2014:51



MASTER'S THESIS 2014:51

# Evaluation of plastic mats as access roads

A study of how plastic mats deform and distribute stress on different soils

*Master of Science Thesis in the Master's Programme Industrial Ecology*

VICTOR GILLHOLM & ISAC ROSANDER

Department of Civil and Environmental Engineering

*Division of GeoEngineering*

*Road and Traffic Research Group*

CHALMERS UNIVERSITY OF TECHNOLOGY

Göteborg, Sweden 2014



Evaluation of plastic mats as access roads to wind farms  
A study of how plastic mats deform and distribute stress on different soils

*Master of Science Thesis in the Master's Programme Industrial Ecology*  
VICTOR GILLHOLM & ISAC ROSANDER

© VICTOR GILLHOLM & ISAC ROSANDER, 2014

Examensarbete / Institutionen för bygg- och miljöteknik,  
Chalmers tekniska högskola 2014:51

Department of Civil and Environmental Engineering  
Division of GeoEngineering  
Road and Traffic Research Group  
Chalmers University of Technology  
SE-412 96 Göteborg  
Sweden  
Telephone: + 46 (0)31-772 1000

Cover:

Figure: PLAXIS 2D analysis for the plastic mat on clay. The Figure is further described in chapter 6.5.4.

Chalmers Reproservice / Department of Civil and Environmental Engineering  
Göteborg, Sweden 2014



Evaluation of plastic mats as access roads to wind farms

A study of how plastic mats deform and distribute stress on different soils

*Master of Science Thesis in the Master's Programme Industrial Ecology*

VICTOR GILLHOLM & ISAC ROSANDER

Department of Civil and Environmental Engineering

Division of GeoEngineering

Road and Traffic Research Group

Chalmers University of Technology

## ABSTRACT

The conventional way of building access roads to wind farms are with gravel roads, which often requires a great amount of material for the embankment. The access roads have special requirements due to heavy transports during the mount and demount of the wind turbine. Modern wind turbines are planned to produce power for approximately 25 years and thus the roads' great capacity will only be needed for a short period of time. The purpose of the thesis is to examine the conditions required to use temporary plastic mats as access roads to wind farms.

The plastic mats are analysed with hand-calculations and a finite element analysis. The hand-calculations are based on a Winkler-model and the general bearing capacity equation that determines the deflection of the mat and the bearing capacity of the soil, respectively. The finite element analysis is performed in the software PLAXIS 2D to investigate the behaviour of the mat for different load and soil cases.

The analysis is conducted to study how different parameters affect the results for the deflection and the bearing capacity. The results show that it is important to determine the soil properties before using the plastic mats. The parameters of consideration are the angle of shearing resistance for the non-cohesive soils, the undrained shear strength for clay, the groundwater level and the effective area of the road mat.

The results show that one of the most sensitive parameter is the effective area and as long as the whole mat area is active the soil is able to handle the load from the transportation for all cases presented. Therefore it is important that the connection system between the mats is able to distribute the load. The calculations in the thesis are based on one detached mat and the area is therefore limited to 3 times 2.5 meters. If the mats are connected to each other and the connections distribute the load, the effective area would be even greater. Thus it is important to further study the connection system to fully understand the behaviour of the plastic mats when they are connected.

Keywords: access roads, plastic mats, shear strength, PLAXIS 2D, Winkler-model, bearing capacity equation, wind farms

Utvärdering av plastmattor som anslutningsväg till vindkraftverk  
En studie om hur plastmattor deformeras och fördelar last på olika jordar  
*Examensarbete i Mastersprogrammet Industrial Ecology*  
VICTOR GILLHOLM & ISAC ROSANDER  
Institutionen för bygg- och miljöteknik  
Avdelningen för Geologi och geoteknik  
Forskargruppen Väg och Trafik  
Chalmers tekniska högskola

## SAMMANFATTNING

Det konventionella sättet att bygga anslutningsvägar till vindkraftverk är med grusvägar, vilka ofta kräver stora mängder material till vägbanken. Anslutningsvägarna dimensioneras efter krav på tunga transporter under montering och demontering av vindkraftverken. Moderna vindkraftverk är planerade att producera elektricitet under 25 år innan de monteras ned., vilket betyder att vägens bärighetskapacitet endast behövs under en kort tidsperiod. Syftet med rapporten är att undersöka de förutsättningar som krävs för att använda tillfälliga plastmattor som anslutningsvägar till vindkraftsparken.

Plastmattorna analyseras med hjälp av handberäkningar och en finit elementanalys. De beräkningar som görs i rapporten baseras på en Winkler-modell och den allmänna bärighetsekvationen för att bestämma nedböjning respektive bärighet hos plastmattan. Finita elementanalysen utförs i programvaran PLAXIS 2D för att bestämma beteendet hos mattan för olika laster och jordar.

Analysen genomförs för att se hur olika parametrar påverkar resultatet för deformation och bärighet. Resultaten visar att det är viktigt att bestämma jordegenskaperna innan plastmattorna kan användas. Parametrarna som studeras är friktionsvinkeln för friktionsjordar, den odränerade skjuvhållfastheten för lera, påverkan av grundvattennivån och den effektiva arean hos mattan.

Resultaten visar att en av de mest känsliga parametrarna är den effektiva arean och så länge som hela mattarean är aktiv kan jorden hantera lasten från transporten för samtliga undersökta fall. Därför är det av största vikt att kopplingen mellan mattorna har förmåga att sprida ut lasten. Beräkningarna i rapporten är baserade på en fristående matta och arean är därför begränsad till 3 gånger 2.5 meter. Om mattorna är anslutna till varandra och kopplingarna kan fördela lasten blir den effektiva ytan större än för en enskild matta. Således är det viktigt att studera kopplingarna vidare för att fullt förstå hur mattorna agerar som en sammankopplad enhet.

Nyckelord: anslutningsvägar, plastmattor, skjuvhållfasthet, PLAXIS 2D, Winkler-modell, allmänna bärighetsekvationen, vindkraftverk

# Contents

ABSTRACT	I
SAMMANFATTNING	II
CONTENTS	III
PREFACE	VI
1 INTRODUCTION	1
1.1 Purpose	1
1.2 Limitations	1
1.3 Method	2
2 ACCESS ROAD TO WIND FARMS	4
2.1 Loads	4
2.1.1 Tire pressure and contact area	6
2.2 Geometric design	7
2.3 Gravel road structure	9
3 TEMPORARY ROADS	11
3.1 Plastic mats	11
3.1.1 TuffTrak	11
3.1.2 Dura-Base	12
3.1.3 MegaDeck	13
3.1.4 Plastic mat properties	13
4 GEOTECHNICAL DESIGN	14
4.1 Soil properties	14
4.1.1 Soil unit weight	15
4.1.2 Shear strength	16
4.1.3 Elastic modulus and Poisson's ratio of different soils	18
4.2 Bearing capacity	20
4.2.1 General bearing capacity equation	20
4.3 California Bearing Ratio (CBR)	23
4.4 Winkler model	24
4.4.1 Infinite beam with concentrated load	26
5 DESCRIPTION OF COMPUTER SOFTWARE	28
6 CASE STUDY	30
6.1 Description of cases	30
6.1.1 Special case	31
6.2 Loads	32

6.3	Bearing capacity	33
6.3.1	Sandy Till	34
6.3.2	Undrained Clay	34
6.3.3	Sand	35
6.4	Deflection of the plate using Winkler model	36
6.5	PLAXIS 2D	37
6.5.1	Distributed load	38
6.5.2	Effective area	38
6.5.3	Sandy Till	39
6.5.4	Clay undrained	40
6.5.5	Sand	41
6.6	Special case	42
7	ANALYSIS	44
7.1	Parametric analysis	44
7.1.1	Bearing capacity	44
7.1.2	PLAXIS 2D	48
7.2	Comparison of PLAXIS 2D with hand-calculations	49
8	DISCUSSION	51
9	CONCLUSIONS	52
10	FURTHER STUDIES	53
11	REFERENCES	54



## Preface

This thesis began with the task to find a new and better solution for access roads to wind farms compared to how they are built today. The solution should require less material and environmental impact than conventional gravel roads. We started to study about access roads to wind farms and eventually we decided to investigate temporary roads. The variety of solutions for temporary roads is great and a lot of work was needed to find suitable products for the wind turbine transportation. Plastic road mats are used as access roads in other industries with heavy transports, thus this product was chosen. The work started with collecting literature on the subject and once gathered we searched for models suitable for calculating the behaviour of the mats. Jorge Yannie was a great support in this search and without him this thesis would not have been possible.

This thesis was made as a research for the company GreenExtreme AB. We would like to thank everyone at GreenExtreme for contributing to the thesis and a special thanks to our supervisor Isabel for always supporting us. We would also like to thanks Miljöbron that made it possible for us to meet with the company.

Last but not least a special thanks to our supervisor Jan Englund at Chalmers for great support.

Göteborg May 2014

Victor Gillholm & Isac Rosander

# 1 Introduction

This thesis started with a company in need of help and two students eager to learn about road construction to wind farms. Roads to wind farms include both the existing road and a newly built site road, which goes under the common name “Access roads”. The conventional site road to a wind farm is made out of gravel, which requires a lot of material for the embankment. This is particularly the case when the upper soil has a low bearing capacity and there is a need to excavate several meters to reach better soil or bedrock. Site roads also impact the landscape and ecosystem depending on the road design and path chosen. The idea of using temporary roads instead of constructing conventional gravel roads is to lower the material usage and the cost of the road construction.

The access road needs to be dimensioned to handle heavy trucks and transportation vehicles during the construction of the wind farm but once constructed it only requires a small road for service and maintenance. The lifetime of a wind turbine is expected to be 25 years and the access roads are normally used by heavy vehicles during the mount and demount of the windmill. For the most of the time the road is therefore oversized and the company wants to see if there is an alternative to the conventional way of constructing roads to reduce both resources and costs. Temporary plastic mats can be the alternative solution, which will be investigated in this thesis.

## 1.1 Purpose

The purpose of the study is to examine the conditions needed to use temporary plastic mats as access roads to wind farms.

To make the purpose clear, several research questions are considered:

Do the plastic mats need a connection system?

Which soil parameters are necessary to investigate before using plastic mats?

How will the mat deflect and distribute the load on different soils?

Is groundwork needed to use plastic mats as access roads?

## 1.2 Limitations

The specifications for the access road used in the study are from the wind turbine manufacturer Vestas. Vestas road specifications are used because it is the only public document available. The specifications from other wind turbine manufactures are similar and thus the result will not be affected by the use of these specifications.

There are several types of temporary roads on the market that may be used for wind turbine transports. In this thesis temporary road in the shape of rectangular road mats made from High Density Polyethylene (HDPE) are studied. The data for the mats are obtained from the manufactures websites.

The modulus of elasticity has not been found for the MegaDeck mat system so it is assumed that the modulus is similar to the one for the DuraBase. This assumption is made due to the fact that these mats are designed with comparable material and that the structure is similar to each other. This assumption may give an error when analysing the MegaDeck mat.

The soil medium is very complex in its nature and the hand-calculations are based on soil with elastic behaviour. This may not reflect the exact behaviour of the soil but it will give an approximation that is comparable to the results from the finite element analysis.

The soil data are general data collected from different literature. For every construction it is crucial to conduct a geotechnical investigation to determine the specific data for the site. Therefore the results from the thesis can be seen as guidelines for different soil properties but proper investigations still need to be undertaken for every specific site.

Calculations are only performed on the TuffTrak mat. This is due to the fact that it is the only one available in Sweden and thus it is the only one that can be implemented by the company at present time. However it is possible to perform the calculations for the other mat systems based on the theory presented in this report.

The cases chosen in the analysis are calculated as one homogenous layer and thus the topsoil, which often includes organic soil, is not taken into account. It is difficult to determine organic soil's strength properties due to inconsistency of the material.

### **1.3 Method**

The literature review on the subject is the primary source of information for this study. The data for the literature review are collected from various sources such as; books, reports, master thesis and websites. Requirements for the access roads to wind farms and specifications on temporary road mats are used for the calculations in the case study.

The case study is separated into two parts; one includes hand-calculations of the bearing capacity and deflection of the mat, while the other part includes a Finite Element Analysis (FEA). The reason for doing both hand-calculations and a FEA is because there is a need to compare the two models to validate if the results from the FEA are reasonable. A homogenous soil layer is used in all cases to be able to compare the calculations. The FEA will be conducted using the software PLAXIS 2D. In addition to the cases a multi-layer case is analysed to investigate how the mat deforms and distribute the stress on very soft topsoil with a dry crust below.

The hand-calculations in the case study are with the Winkler model and the general bearing capacity equation. The Winkler model is used to determine the deflection of the mat on different soils while the bearing capacity equation is used to determine if the soil can handle the pressure from the load. The results from the hand-calculations are then compared to the results from the analysis in PLAXIS 2D.

The finite element analysis is conducted in the software PLAXIS 2D, which is specialised for geotechnical engineering. The software can be used to analyse deformations, stability and stresses in the soil. In PLAXIS 2D it is possible to use features to analyse the interaction between a structural element and the soil to determine how the soil and mat behaves when a load is applied.

In the analysis a parametric study is conducted to determine how the soil properties affect the results. This is made both for the hand and computer calculations. A comparison between the results is performed to validate the correlation between the models.

In Figure 1.1 an overview of the method is presented to make it easier to understand the working process and how the thesis is conducted.

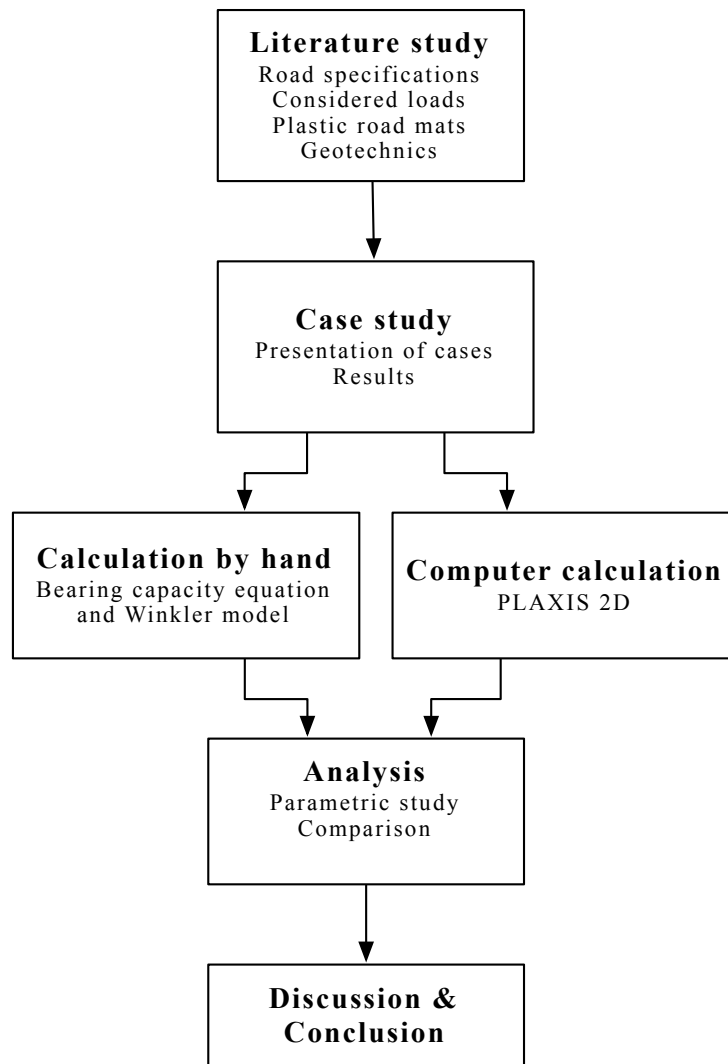


Figure 1.1 Method chart – description of how the thesis is conducted

## 2 Access road to wind farms

The access road needs to be dimensioned to handle heavy vehicles and great loads. During the mount of the wind turbine heavy trucks need access to the site for transports of wind turbine components. Wind turbine manufacturers have different requirements for the access road in terms of minimum bearing capacity, curve radius, maximum inclination and width. Typically the width requirement varies between 3 and 9 meters depending on manufacturer and site conditions (BLM, 2005).

Road specifications from wind turbine manufacturers are generally published as a classified document. However, guidelines from Vestas 1.8 - 3 MW turbines are public and therefore used in this thesis (Vestas, 2010).

### 2.1 Loads

The access road and site road to a wind farm needs to be dimensioned for heavy loads during the construction of the foundation and later to handle heavy transport vehicles carrying wind turbine components. In road design, the loads are described as maximum allowable axle load and number of standard axles.

Axle load is defined as the load that one axle of a vehicle transfers to the road. The axle load is spread to the road from a single or dual configuration of wheel pairs, depending on the design of the vehicle. A standard axle load in Sweden is defined as a single axle carrying a load of 100 kN as seen in Figure 2.1 (Andersson, 2011)

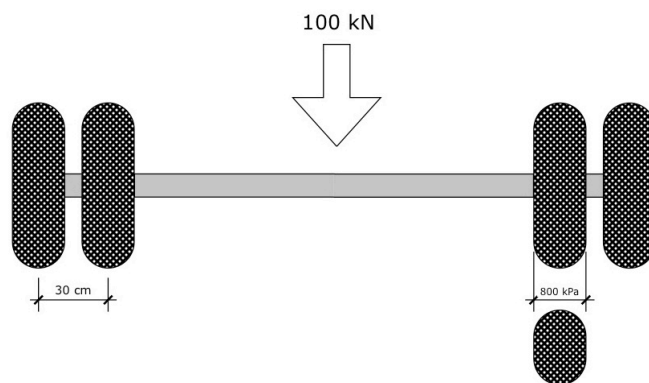


Figure 2.1 A standard axle carrying 100 kN with a tire pressure of 800 kPa (Based on Andersson (2011))

When designing roads it is important to estimate the traffic load that road will encounter during its technical lifetime. Standard axles are thus used to sum up the total traffic that the road needs to support. Equation (2.1.1) presents the calculation procedure for the amount of standard axles,  $N_{ekv}$ , when designing roads (Andersson, 2011).

$$N_{ekv} = \dot{A}DT_k \cdot 3.65 \cdot A \cdot B_{just} \cdot \sum_{j=1}^n \left(1 + \frac{k}{100}\right)^j \quad (2.1.1)$$

The variables in equation (2.1.1) depends on annual daily traffic in one traffic lane or direction ( $\dot{A}DT$ ), ratio of heavy vehicles ( $A$ ), justified standard axles per heavy vehicle

( $B_{just}$ ), intended period of dimension in year ( $n$ ), the change of heavy traffic load in percentage per year ( $k$ ) and ( $j$ ) which is a series of number from 1 to  $n$ .

The total standard axles on a site road during construction of a wind farm could be predicted with more precision than a general road. This is because the number of transports and specific vehicles needed for the construction is known.

In Trafikverket's report 2010:032, expected transports to windmills during construction are presented. Windmills with concrete foundation may generate 50 to 100 transports with concrete mixer trucks. The total load and axial pressure of the concrete trucks are adjusted with the allowable bearing capacity of the access roads, thus the total amount of concrete transports may differ for identical concrete foundations. The heaviest and largest transport vehicles are those with wind turbine and crane parts. As an example Vestas 2.0 MW turbine is split into 10 transport modules varying in both length and weight, see Table 2.1.

Table 2.1. *Specific transport measures of wind turbine components (Nilsson, 2010).*

Model	MW	Turbine part	Loaded transport vehicle measure			
			Length [m]	Width [m]	Height [m]	Weight [ton]
Vestas	2.0	Mounting plate	4.7	4.7	4.0	40
		Blade	49	3.4	4.0	40
		Nacelle	34	4.3	4.3	125
		Rotor	17	3.6	4.2	48
		Bottom tower section	48	4.2	4.3	123
		Middle tower section (1)	50	4.2	4.3	104
		Middle tower section (2)	30	3.3	4.2	70
		Top tower section	27	3.3	4.2	56

As seen in Table 2.1, the nacelle is the heaviest transport module and has a total load of 125 tons. With respect to transportation, the bottom tower section is the most critical module because of its heavy weight and length (Hau, 2013). The road is thus designed to meet the heaviest possible total load and axial load. Vestas document on road specification for 1.8-3.0 MW turbines requires the road to handle a minimum axle load of 17 tons (Vestas, 2010).

### 2.1.1 Tire pressure and contact area

The greatest axle load on a wind turbine transport is normally on the rear axles on the trailer where dual tires are used to spread the load to the road surface (Nilsson, 2010). Tandem and tridem axles are normally used on semi-trailers for heavy-duty haul trucks, however flatbed trailers carrying heavy loads could have several more axles to spread the load (Huang, 2004).

It is necessary to know the contact area between the tires and the road surface to be able to assume the area that the axle load will be uniformly distributed over. The contact pressure of a tire could be seen as a rectangular area with two semicircles at the edges. The actual area of the tire pressure could be transformed to an equivalent rectangular area using equation (2.1.2) (Huang, 2004).

$$L = \sqrt{\frac{A_C}{0.5227}} \quad (2.1.2)$$

In equation (2.1.2),  $L$  is the length of the contact area in the tire's driving direction and  $A_C$  is the contact area, which can be obtained by dividing the load on the specific tire by the tire pressure. The suggested equivalent rectangular area has one side with the length  $0.8712L$  and another side with  $0.6L$ . In Figure 2.2, the actual contact area and the transformed rectangular area are presented. The problem is that this area could not be used within layered theory for flexible pavement, because of the area not being axisymmetric (Huang, 2004).

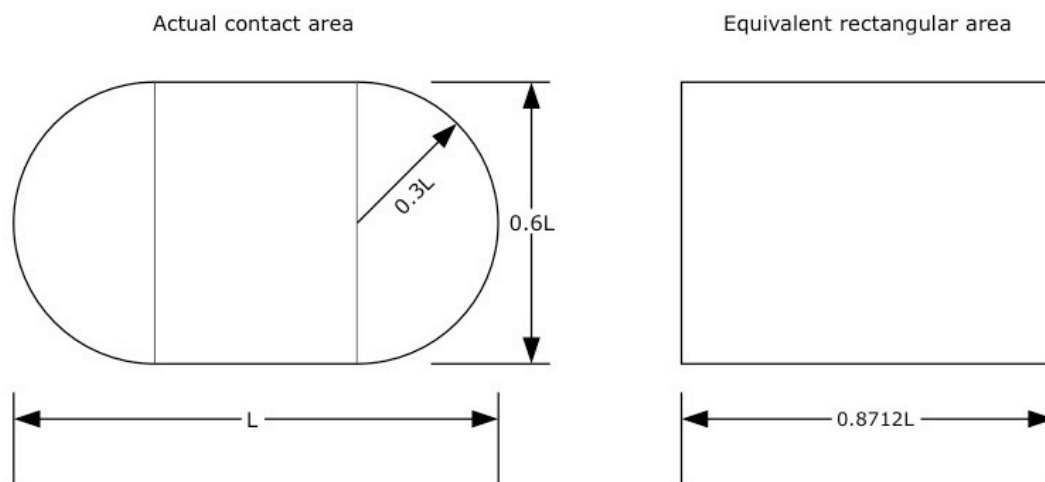


Figure 2.2 Contact area and equivalent rectangular area from a tire. (Based on Huang, 2004)

For flexible pavement design it is assumed that the tire has a circular contact area and to make the analysis easier it is also common to combine the two circle areas for dual tires as one larger circle.

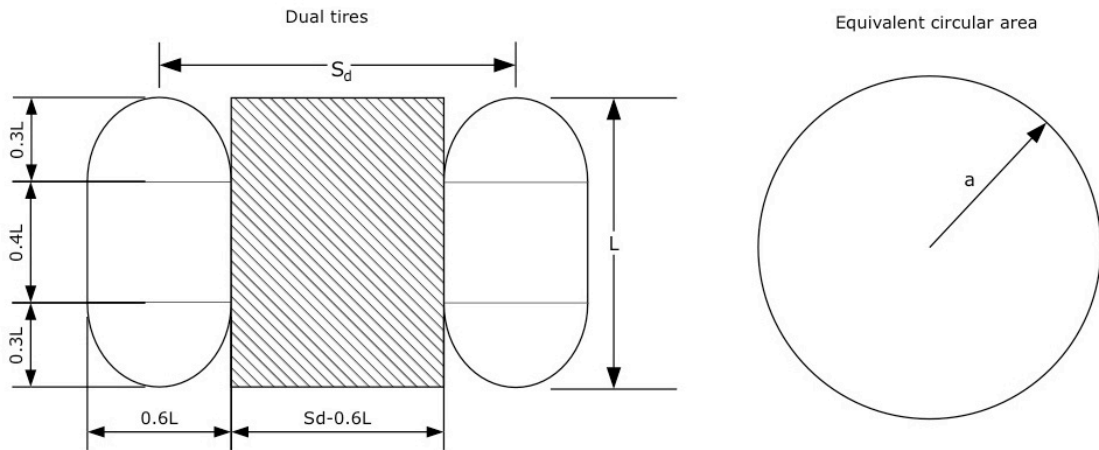


Figure 2.3 Dual tires' contact area transformed to a circle with radius  $a$ . (Based on Huang, 2004)

Figure 2.3 above illustrates how dual tires' contact area could be interpreted as one large circle. The circle's total contact area contains the tires' areas plus the area between the duals. It has been shown that one larger circle gives a more approximate result in calculations than two separate circles (Huang, 2004).

$$\frac{P_d}{q} = \pi(0.3L)^2 + (0.4L)(0.6L) = 0.5227L^2 \Rightarrow L = \sqrt{\frac{P_d}{0.5227q}} \quad (2.1.3)$$

Equation (2.1.3) describes the area of one tire where  $P_d$  is the load on the tire and  $q$  is the contact pressure, equal to the tire pressure. The area of an equivalent circle can be calculated using equation (2.1.4).

$$\pi a^2 = 2 \times 0.5227L^2 + (S_d - 0.6L)L \quad (2.1.4)$$

When inserting  $L$  from equation (2.1.3) in (2.1.4), it yields the total area of an equivalent circle.

$$\pi a^2 = \frac{0.8521P_d}{q} + S_d \sqrt{\frac{P_d}{0.5227q}} \quad (2.1.5)$$

where

$P_d$  Load on tire [N]

$q$  Contact pressure, Tire pressure [Pa]

$S_d$  Distance between tires in dual configuration [m]

$\pi a^2$  Area of the circle [m<sup>2</sup>]

## 2.2 Geometric design

Existing roads and site roads must fulfil specific geometric requirements to be able to transport wind turbine parts to the site. The elements to consider in the geometric design are the horizontal alignment, vertical alignment and cross-section (Robinson, 2004).

Access and site roads have specific radius requirements for horizontal curves due to great length of transport vehicles. The transports could be up to 50 meters (see Table 2.1), which requires the horizontal bends to have a sufficient radius to be able to make the turns. The intersection from a public road to a site road needs to be modified for long transport vehicles. If the connection is 90 degrees to the public road an inner radius of 43 meters is recommended (Vestas, 2010).

The vertical alignments of the road consider the longitudinal radii and gradient required for transports to the wind farm (Robinson, 2004). The longitudinal radii for both convex and concave curves must be more than 200 meters for Vestas 1.8 – 3.0 MW turbines (Vestas, 2010). In Figure 2.4 the longitudinal radius is presented for convex and concave vertical curves. The limitation of the radius is for safety reasons due to the fact that smaller radius may risk the transportation of the wind turbine components (Vestas, 2010).

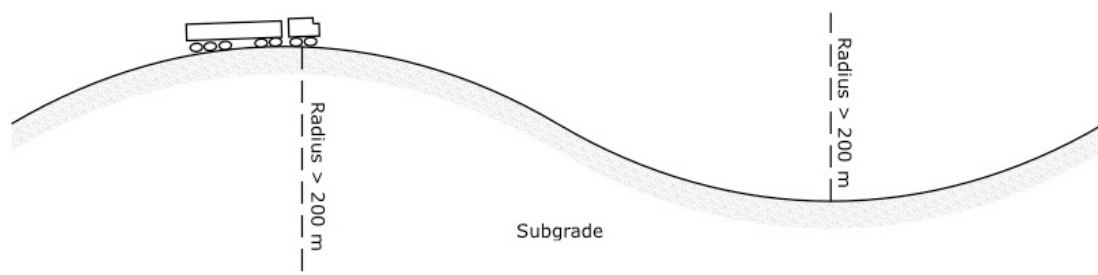


Figure 2.4 The longitudinal radii for convex and concave curves (Based on Vestas, 2010)

The longitudinal gradient is a measurement for the inclination of the road. The inclination is usually presented as percentage or as 1: n (Andersson, 2000). Equation (2.2.1) and Figure 2.5 presents the relation between the inclination and the angle.

$$i = \tan \varphi = 1:n \quad (2.2.1)$$

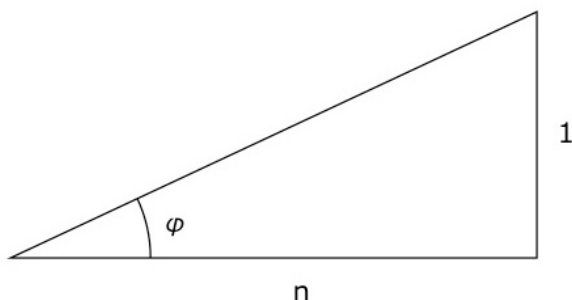


Figure 2.5 The relation between the angle and the inclination

The longitudinal gradient of the road should not exceed 8 degrees for the transportation of the windmill component. The lateral gradient must be a maximum of 2 degrees, see Figure 2.6 (Vestas, 2010). The restriction for both the lateral and the longitudinal gradient is due to the fact that steeper inclinations will danger the transportation of the wind turbine parts.

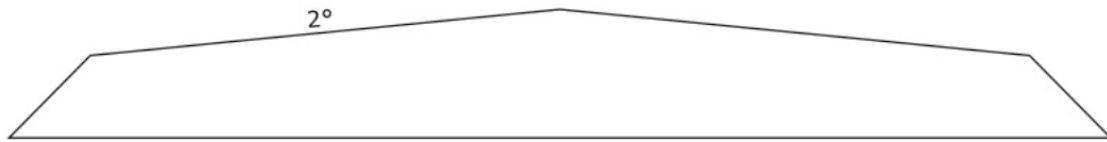


Figure 2.6. Cross section of a road with lateral gradient of 2 degrees

As mentioned before it is important that the lateral gradient of the road is not too steep but an inclination is necessary for the water runoff. Without an inclination the water will gathered on the surface causing abrasion on the road (Robinson, 2004).

### 2.3 Gravel road structure

Gravel roads are the conventional solution for access roads to wind farms. The road needs to be dimensioned for axial loads up to 17 tons (Vestas, 2010). A typical cross section is presented in Figure 2.7.

The road structure aims to support the traffic and transmit the load to the soil below. The structure reduces the stress to the point where the soil can bear the load. Consequently it is the subgrade properties that determine the required thickness of the road structure (Robinson, 2004).

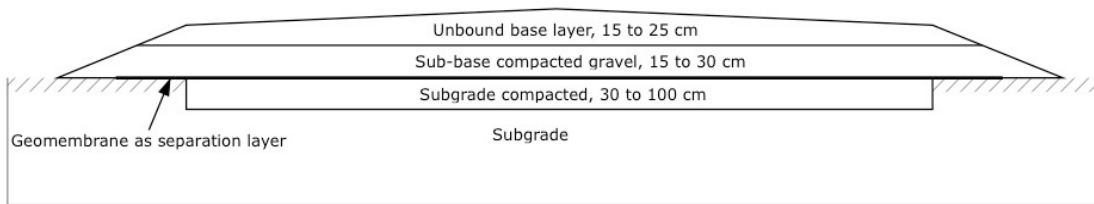


Figure 2.7 Cross section of a gravel road (Based on Robinson, 2004)

The material used for gravel roads needs to have requirements in terms of bearing capacity and moisture retention properties. A gravel road is constructed in several layers; subgrade, sub-base and unbounded base layer (Robinson, 2004). The road is constructed with a crowned driving surface to prevent water to accumulate on the road surface (VTI, 2014). The subgrade consists of the underlying soil and if necessary fill-material transported to the site. The subgrade is acting as a foundation for the road and therefore a geotechnical investigation is required before constructing the road to determine the bearing capacity of the soil (Robinson, 2004). The sub-base layer distributes the load and is operating as a separation layer between the subgrade and the base. It is also common to use a geomembrane under the sub-base as a separation layer to avoid material erosion. The sub-base is usually constructed with natural gravel and works as a platform during the construction of the upper layers. The unbounded base layer is where the main load spreading occurs (Robinson, 2004).

The chosen inclination on slopes of the embankment depends on soil properties, topography and the importance of the road. Robinson states that most soil types are stable at slopes of 1:1.5. The earthwork will decrease with steep slopes but the risk of erosion increases due to higher water velocity (Robinson, 2004). Thus it is important to consider the cost of earthwork versus the cost of future maintenance. VTI suggest that the slope inclination should be 1:1.5 on the outer embankment and 1:3 on the

inner embankment. The ditch provides drainage for the road and a functional drainage with a proper cross fall are important for the road to function correctly (VTI, 2014).

According to Vestas road specifications, the road needs to be constructed so that the maximum irregularities on the surface do not exceed 150 mm on a length of 30 meters. Vestas further states that the site road should have a California Bearing Ratio (CBR) of more than 60 % to be able to withstand the loads (Vestas, 2010). CBR is further described in chapter 4.3

### 3 Temporary roads

Temporary road is a term including many types of solutions for accessing construction sites. Steel, aluminium, wood and plastic are just a few of the materials that are being used around the world. Temporary roads are used in many industries such as; oil and gas, building and construction and the forest industry to get access to rural areas.

#### 3.1 Plastic mats

Road mats made of plastics are a fairly new product on the market. Thus, there have not been many independent studies conducted on the mats and most of the data in this chapter has been collected from the manufactures websites. There are mainly three plastic road mats on the market for heavy-duty vehicles; TuffTrak, MegaDeck and Dura-Base.

##### 3.1.1 TuffTrak

TuffTrak heavy-duty road mat is made from High Density (HD) or Ultra High Molecular Weight (UHMW) polyethylene. TuffTrak has the dimensions of 3 times 2.5 meters and a solid design with a core thickness of 38mm. Due to the solid design of the TuffTrak the risk of cross contamination is minimized. The mat weighs 290 kg, which enables less transportation, compared to conventional steel plates. Zigma ground solutions Ltd is the company behind the product and according to them the mat can support loads up to 150 tonnes (Zigma ground solutions, 2014).



*Figure 3.1 TuffTrak road mat (Zigma ground solution, 2014)*

The TuffTrak has a dual grip design with a chevron traction surface on one side and a low profile traction surface on the other. The chevron traction surface is designed with broken pattern of rugged nubs, which improves the grip for heavy vehicles. The chevron surface shall therefore be used for the heavy-duty transportation while the low profile side is more suitable for example storage areas. (Zigma ground solutions 2014)

There are two different types of connections used for the TuffTrak mat system, the metal connector and Orange Hi Viz Flex connector. The metal connector should be used for most conditions and vehicles while the Orange Hi Viz Flex connector should be used where the ground is highly uneven.

The Young's modulus of elasticity is 900 MPa for the TuffTrak and the Poisson's ratio is 0.35 (Zigma ground solutions, 2014).

### 3.1.2 Dura-Base

The Dura-Base composite mat is made from High Density (HD) polyethylene. The mat is in total 2.44 times 4.27 meters including the interlocking edges and the thickness is 10.8 centimetres. However the useable area without the overlapping edges is 3.96 times 2.13 m. The Dura-Base weighs 454 kg but the weight may increase to about 700 kg if water enters the mat (Maybehire, 2007). The interlocking system with the overlaying edges allows the mats to distribute the load over a large surface area to the ground.



Figure 3.2. Dura-base road mat (Newpark Resources, 2014)

The interlocking system of the Dura-Base has sixteen slots per mat, which allows a variety of different configurations. The number of locking pins required depends on the soil conditions at the site and hence the number of locking pins should be increased when the bearing capacity of the soil decreases. The load capacity according to the company Newpark Resources Inc. is  $40 \text{ kg/cm}^2$ , which corresponds to around 3920 kPa (Newpark Resources, 2014).

The preparation needed for the site is minimal to none but the site needs to be relatively flat. The mat system could handle 150-200 mm variation over 1.2 m but it is important that there are no sharp objects under the mat that may cause locally mat crush. To eliminate the risk of damage on the mat a sub-base layer of ballast may be required (Maybehire, 2007). According to Gonzalez (2010), the modulus of elasticity and the Poisson's ratio are 462 MPa and 0.3, respectively.

### 3.1.3 MegaDeck

The MegaDeck composite mat is made from High Density (HD) polyethylene and the size is 4.27 times 2.28 meters with a thickness of 10.8 centimetres. Due to the overlapping edges, the usable area is 3.96 times 1.81 meters. The mat is designed with an interior ribbed structure and the total weight of the mat is 476 kg (Megadeck, 2014). MegaDeck mats have interlocking edges on both sides, which allow the mats to be easily connected to other panels. The connecting system consists of aluminium pins and is inserted in the holes in the overlapping edges, which provide strength and rigidity at the joints. According to the company's website the MegaDeck can handle compressive loads up to 600 psi, corresponding to around 4100 kPa, over ideal soil conditions. The MegaDeck mats are designed with an anti-slip traction pattern, which gives traction to all form of vehicles (Megadeck, 2014).

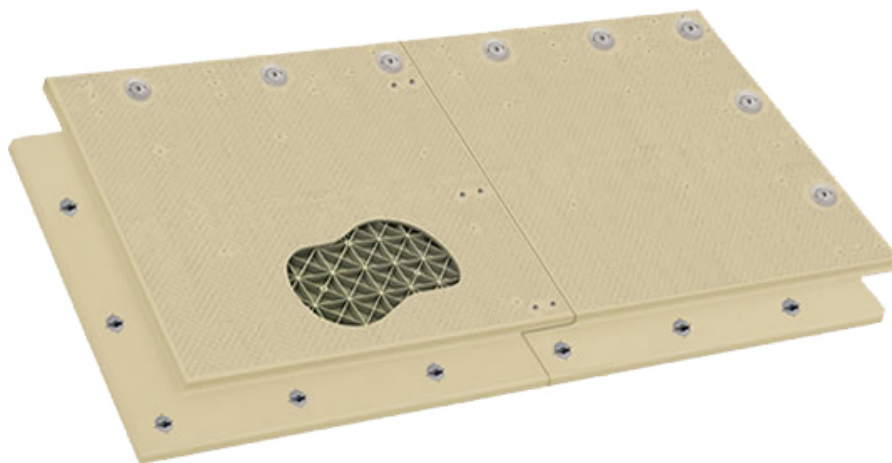


Figure 3.3 MegaDeck road mat (Megadeck, 2014)

According to a Finite element analysis conducted of the company Signature Fencing & Flooring the MegaDeck can support loads up to 178 kN in soil conditions corresponding to soft clay (CBR 2) (Harry, 2010). The modulus of elasticity is as can be seen in the limitations assumed to be the same as the one for the Dura-Base, 462 MPa. The Poisson's ratio of the MegaDeck mat system is 0.3.

### 3.1.4 Plastic mat properties

The mats properties and measures have been summarised in Table 3.1.

Table 3.1 Properties of different plastic road mats on the market

	Dimensions [m] (Usable area)	Weight [kg]	Elasticity [MPa]	Poisson's ratio [-]
TuffTrak	3 x 2.5 x 0.038	290	900	0.35
Dura-Base	4 x 2.1 x 0.108	454	462	0.3
MegaDeck	4 x 1.8 x 0.108	476	462	0.3

## 4 Geotechnical design

For civil engineering works, such as roads and buildings, it is important to determine the ground conditions beneath the structure. This is important because the soil needs to support the expected loads from the structure above to avoid collapse, settlements and other failures. The part of the structure that transmits the load directly to the underlying soil is called a foundation, thus a road could be defined as a foundation. The process where the applied load on foundations transfers to the ground is called soil-structure interaction (Craig, 2012). The soil together with the foundation seen as one rigid body is called geostructure.

Different design codes are developed to ensure that the design of the structure is made in the correct manner. The structure is often designed to meet two principal performance requirements, called Ultimate limit states (ULS) and Serviceability limit states (SLS) (Craig, 2012). ULS ensure that the foundations capacity or resistance is sufficient to support the loads applied and SLS to avoid excessive deformation, which might lead to function loss or damaging of the structure. In Sweden the Swedish Standard Institute, SIS, has developed a standard for geotechnical design called SS-EN1997 Eurocode 7. This code mentions several types of failures that one need to take into account when designing structures on ground. The Ultimate limit states (ULS) in Eurocode 7 are the following (SIS, 2008):

- Overall equilibrium in the geostructure (EQU)
- Internal failure or excessive deformation of the structure (STR)
- Failure or excessive deformation of the ground (GEO)
- Loss of equilibrium of the geostructure due to uplift by water pressure (UPL)
- Hydraulic heave or internal erosion caused by hydraulic gradients (HYD)

Eurocode 7 is also recommending safety factors for soil parameters and bearing capacity.

### 4.1 Soil properties

The most common soil in Sweden is till and it covers 75% of the land area. The till consists of different fraction with everything between clay and boulders (Nilsson, 2003). Glaciofluvial deposits, fine-grained sediment and peat lands cover 15% and the last 10% is exposed bedrock and soil with less depth than half a meter over bedrock.

Soils can be divided into three different main categories; non-cohesive, cohesive and organic soils. Non-cohesive soil, also called coarse-grained soils, varies in size from boulders to fine sand and is typically stable and well suited as foundations (Kendrick et al 2004). Cohesive soils include different type of clays, marls and silts. These soils are more liable to deform and plasticise under loads compared to non-cohesive soils. Cohesive soils are also likely to deform due to frost actions or change in moisture content. Organic soils are soils with high organic content such as topsoil and peat. The deformations under loading are generally great on these soils (Kendrick et al, 2004).

Soil is a complex medium that behaves neither elastic nor plastic. In spite of this the elasticity theory has been shown to give good estimations on deformations when compared to measured values (Larsson, 2008).

Soil matters have different properties that vary with the material and how it is arranged in the ground. Soil material can be defined as a three-phase material that consists of solids, water and void space. A phase diagram that views the relation between solids, water and air is seen in Figure 4.1 below. The solids, for example grains or particles, form a soil-skeleton that supports the own weight and also distributes loads through the soil (Sällfors, 2009).

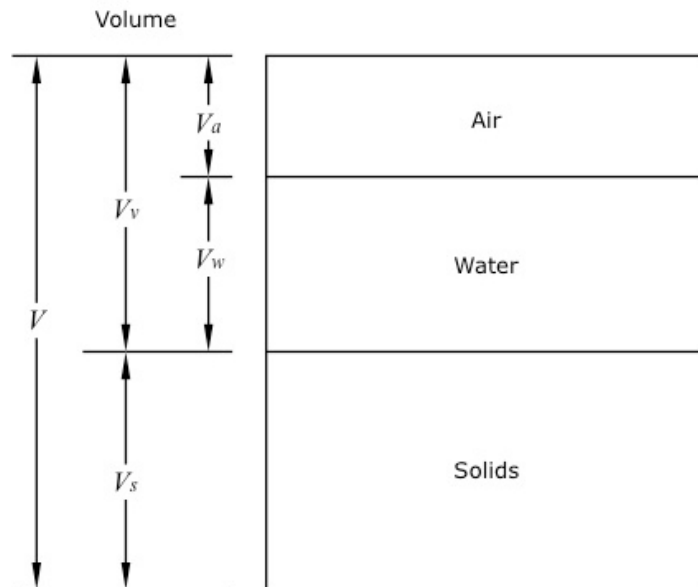


Figure 4.1 Phase diagram of soil (Based on Craig, 2012)

#### 4.1.1 Soil unit weight

Soil has different density depending on the water content, solids and voids. The unit weight ( $\gamma$ ) of the soil is the density multiplied with gravity, which is usually expressed in  $\text{kN/m}^3$ . The general formula is described below in equation (4.1.1). (Craig, 2012)

$$\gamma = \frac{M}{V} g = \rho g \quad (4.1.1)$$

A more detailed formula that illustrates how the water content, voids and solids affect the unit weight is described in equation (4.1.2).

$$\gamma = \frac{\left(\frac{\rho_s}{\rho_w}\right) + S_r e}{1 + e} \gamma_w \quad (4.1.2)$$

where

$\rho_s$  density of solids [ $\text{kg/m}^3$ ]

$\rho_w$  density of water [ $\text{kg/m}^3$ ]

$S_r$  degree of saturation, the ratio between water and void space [-]

$e$  void ratio, volume of voids to the volume of solids [-]

$\gamma_w$  unit weight of water [ $\text{kN/m}^3$ ]

In Table 4.1 below typical values for different soil materials are shown. It is always preferable to determine the unit weight of a specific soil through soil investigations at the site (Bergdahl, 1993), but when data is missing low approximate values could be used.

Table 4.1 Typical unit weights of soils (Based on Larsson, 2008)

Soils unit weight [kN/m <sup>3</sup> ]	Saturated soil	Effective unit weight under groundwater level	Naturally moisturised soil
	$\gamma_{\text{sat}}$	$\gamma'$	$\gamma_m$
Crushed rock	21	11	18
Macadam	21	11	18
Gravel	22	12	19
Gravel Till	23	13	20
Sand	20	10	18
Sandy Till	22	12	20
Silt	19	9	17
Silt Till	21	11	20
Clay	17	7	17
Clayey Till	22	12	22
Gyttja	14	4	14
Peat	11-13	1-3	11-13

#### 4.1.2 Shear strength

Mohr-Coulomb model is often used to define shear strength at different effective stresses in soils. This model will not be derived, only the basics needed to understand that soils have different properties. Shear strength is easiest described as the maximum shear stress the soil can sustain before failure. The shearing resistance is developed mechanically due to inter-particle contact forces and friction.

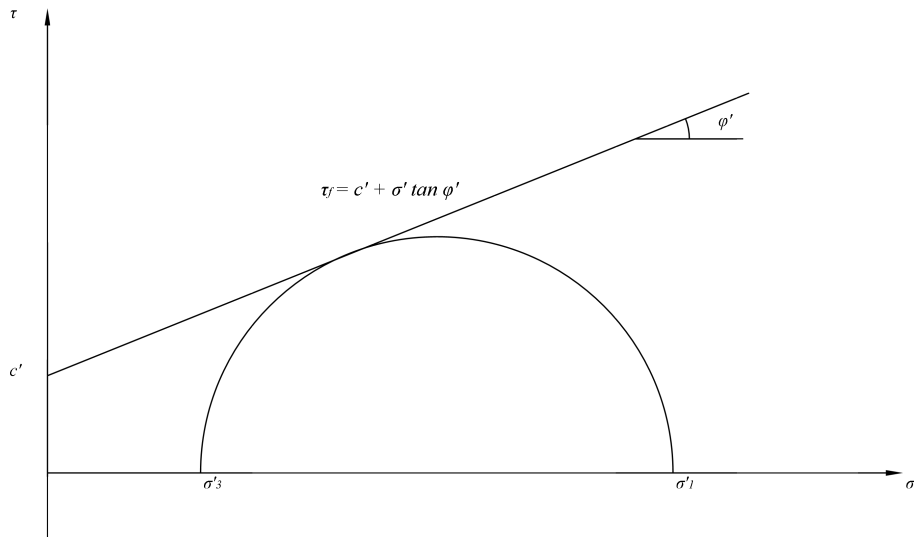


Figure 4.2 Mohr-Coulomb failure envelope (Craig, 2012)

Figure 4.2 and Equation (4.1.3) present the Mohr-Coulomb's failure envelope, which is an approximation of the shear strength depending on the cohesion intercept,  $c'$ , the angle of shearing resistance,  $\varphi'$  and the effective stress,  $\sigma'$  (Craig, 2012). For undrained cohesive soil conditions the Mohr-Coulomb's failure envelope above is instead a straight horizontal line, because the absence of the angle of shearing resistance.

$$\tau_f = c' + \sigma' \tan \varphi' \quad (4.1.3)$$

where

- $\tau_f$  shear strength [Pa]
- $\sigma'$  effective shear stress [Pa]
- $c'$  cohesion [Pa]
- $\varphi'$  angle of shearing resistance [°]

Cohesion can be defined as the independent strength to resist a force trying to deform or hold the solid together. In Figure 4.2 the cohesion is where the shear strength intersects with the y-axis showing the independences of an increased shear stress. This strength is due to negative pore pressure in the void spaces and cementation of soil particles (Craig, 2012). When a cohesive soil is loaded the pore pressure initially carries the stresses, successively as water drains from void spaces the soil change state from undrained to drained. Over time the soil will lose almost all of its cohesion and the soil skeleton will carry the stresses instead. This leads to decreases in volume and is called consolidation and results in settlements (Sällfors, 2009).

Angle of shearing resistance is the angle that the shear strength increases due to stresses. The soil's cohesion and angle of shearing resistance are normally determined through specific geotechnical investigations (Sällfors, 2009), but approximate values for the angle of shearing resistance are detailed in table 4.2.

Table 4.2 Typical angle of shearing resistance for soils based on geotechnical data (Sällfors, 2009).

Degree of compaction	Silt	Sand	Gravel	Sandy Till	Gravelly Till	Macadam	Crushed rock
Low	26°	28°	30°	42°	38°	30°	40°
High	33°	35°	37°	45°	45°	38°	45°

The shear strength for undrained cohesive soil is independent of the angle of shearing resistance and different values are presented in Table 4.3 below (Sällfors, 2009). Clayey soils have often developed a dry crust near the surface with higher shear strength than the layers below. The thickness of the dry crust can vary from less than a meter to several meters.

Table 4.3 Undrained shear strength of cohesive soils (Larsson, 2008)

Strength	Undrained shear strength, $c_u$ [kPa]
Extremely low	<10
Very low	10-20
Low	20-40
Medium	40-75
High	75-150
Very high	150-300
Extremely high	>300

According to Sällfors the cohesion for drained cohesive soils can be assumed to be 10 percentage of the undrained shear strength,  $c_u$  and the angle of shearing resistance 30° (Sällfors, 2009).

### 4.1.3 Elastic modulus and Poisson's ratio of different soils

Soil is a complex medium that behaves neither elastic nor plastic. In spite of this the elasticity theory has been shown to give good estimations on deformations when compared to measured values (Larsson, 2008). Typical modulus of elasticity for different soils is presented in Table 4.4 (Subramanian, 2010).

Table 4.4 Modulus of elasticity for different soils (Subramanian, 2010)

Soil	Type	Modulus of Elasticity, E [MPa]
Till	Loose	10-153
	Dense	144-720
	Very dense	478-1440
Clay	Very soft	2-15
	Soft	5-25
	Medium	15-50
	Hard	50-100
	Sandy	25-250
Sand	Silty	7-21
	Loose	10-24
	Dense	48-81
Sand and gravel	Loose	48-148
	Dense	96-192
Shale	-	144-14400
Silt	-	2-20

The elastic modulus of the soil is used in different models to calculate the deflection and stresses of the soil. The elastic modulus can be determined by performing geotechnical investigations (Sällfors, 2009).

Poisson's ratio is defined as the ratio between the lateral strain and the longitudinal strain, when the applied stress is uniaxial (Bowles, 1977). The Poisson's ratio differs for every soil, for approximate values see Table 4.5.

Table 4.5 Typical values for Poisson's ratio (Bowles, 1977).

Type of soil	Poisson's ratio
Clay, saturated	0.4-0.5
Clay, unsaturated	0.1-0.3
Sandy clay	0.2-0.3
Silt	0.3-0.35
Sand (Dense)	0.2-0.4
Sand (Coarse)	0.15
Sand (Fine grained)	0.25
Rock	0.1-0.4

## 4.2 Bearing capacity

Soils have different properties to support loads and one common measure to describe this is to determine their bearing capacity ( $q_f$ ), which is defined as the pressure that causes shear failure under, and adjacent to a foundation (Craig, 2012). The general bearing capacity equations is an Ultimate Limit State calculation and could be used for example foundations and plates.

### 4.2.1 General bearing capacity equation

The bearing capacity of a soil could be estimated with the general bearing capacity equation described by Terzaghi. To be able to calculate the bearing capacity one must know the angle of shearing resistance for the soil ( $\varphi$ ), the soil average unit weight ( $\gamma$ ) and the cohesion ( $c$ ). These parameters could be determined by in-situ tests or in laboratories. The equation depends on three different terms each contributing to the total bearing capacity (Terzaghi, 1967).

$$q_f = q_c + q_q + q_\gamma$$

The first term (1) depends on the cohesion and friction of a weightless material carrying no surcharge load.

$$(1) q_c = cN_c$$

The second term (2) depends on the friction of a weightless material with a surcharge load  $\sigma$  on the ground surface. The load  $\sigma$  could also be described as the weight of the soil ( $\gamma$ ) and the depth ( $D_f$ ) above the footing. If the footing is placed on the ground surface with no surcharge load this term can be neglected.

$$(2) q_q = \gamma D_f N_q = \sigma_q N_q$$

The third term (3) describes the friction of a material with a weight and carrying no surcharge. The variable  $B$  depends on the width of the footing and with this form it is assumed that the footing is continuous.

$$(3) q_\gamma = \frac{1}{2} \gamma B N_\gamma$$

These terms together describe the general bearing capacity of a soil, which can be expressed as

$$q_f = cN_c + \sigma_q N_q + \frac{1}{2} \gamma B N_\gamma \quad (4.2.1)$$

where

$N_q$  bearing capacity factor depending on surcharge load

$N_c$  bearing capacity factor depending on the cohesion

$N_\gamma$  bearing capacity factor depending on weight of the soil under the footing

There are several different equations for the bearing capacity factors to choose from, which all gives similar values. The bearing capacity factor  $N_q$ ,  $N_c$ ,  $N_\gamma$  based on the angle of shearing resistance is calculated with the following equations (Craig, 2012).

$$N_q = \frac{1 + \sin \phi'}{1 - \sin \phi'} e^{\pi \tan \phi'} \quad (4.2.2)$$

$$N_c = \frac{N_q - 1}{\tan \phi'} \text{ when } \phi' > 0 \text{ and } \pi + 2 \text{ when } \phi' = 0 \quad (4.2.3)$$

$$N_\gamma = 2(N_q - 1) \tan \phi' \quad (4.2.4)$$

Equation (4.2.1) is valid when the following assumptions are made (Sällfors, 2009):

- The width ( $B$ ) of the foundation is constant
- The foundation is considered as elongated
- The foundation is placed on a horizontal surface
- The foundation has a surcharge load
- The weight of the soil is  $\gamma$
- The soil is considered as homogenous with the constant parameters  $c$  and  $\phi$
- The load is vertical and centric of the foundation

Several correction factors are empirically developed for other cases than the assumed conditions in the list above. These factors are multiplied to each term in the equation and depend on the shape of the foundation, depth of the foundation, inclined load and surface, eccentricity load and the impact of ground water level (Sällfors 2009). With the correction factors added the bearing capacity equation gets the following appearance

$$q_f = cN_c s_c d_c i_c g_c + \gamma D_f N_q s_q d_q i_q g_q + \frac{1}{2} \gamma' B_{ef} N_\gamma s_\gamma d_\gamma i_\gamma g_\gamma \quad (4.2.5)$$

where

$q_f$	the bearing capacity of the foundation/plate [Pa]
$c$	the cohesion of the soil [Pa]
$B_{ef}$	the effective width depending on eccentricity [m]
$\sigma_q$	the surcharge load at surface level [Pa]
$\gamma'$	the effective unit weight of the soil [ $\text{kg/m}^3$ ]
$N_c, N_q, N_\gamma$	bearing capacity factors [-]
$s_c, s_q, s_\gamma$	correction factor depending on the shape of foundation [-]
$d_c, d_q, d_\gamma$	correction factor depending on the foundation depth [-]
$i_c, i_q, i_\gamma$	correction factor depending on inclined load [-]
$g_c, g_q, g_\gamma$	correction factor depending on inclined ground surface [-]

If the load is applied outside the geometric centre, the resultant of the ground pressure changes and thus the effective width ( $B_{ef}$ ) and length ( $L_{ef}$ ) should be used (Bergdahl et al, 1993). The effective width and length and the resulting area are calculated with

$$\begin{aligned}
 B_{ef} &= B - 2e_B \\
 L_{ef} &= L - 2e_L \\
 A_{ef} &= B_{ef}L_{ef}
 \end{aligned}
 \tag{4.2.6}$$

Where  $e_B$  and  $e_L$  is the distance from the geometric centre as seen in Figure 4.3.

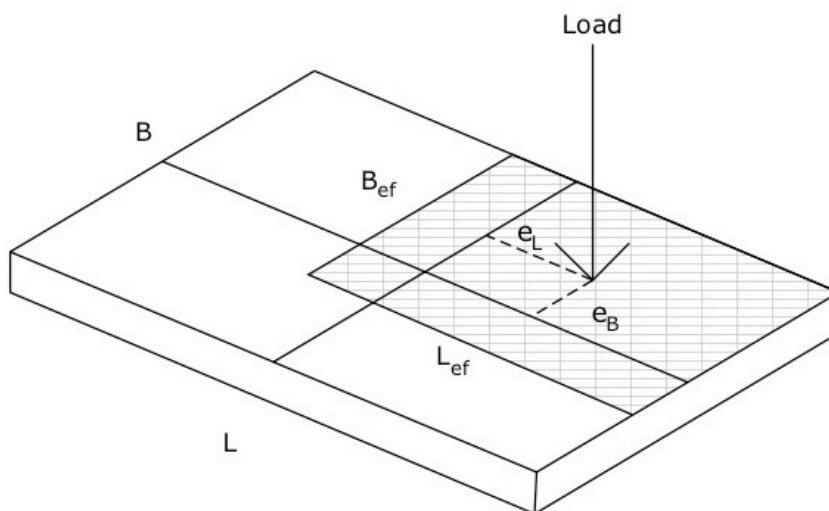


Figure 4.3 The effective width and length of a plate with an eccentric load applied. (Inspired from Bergdahl et al, 1993)

The shape factors  $s_c, s_q, s_\gamma$  depend on the shape of the foundation and the angle of shearing resistance in the soil. The shape factors have been developed from accurate

limit analyses (Craig, 2012). It is recommended in Eurocode 7 to use the following expression for the shape factors (where  $B < L$ )

$$s_q = 1 + \frac{B}{L} \sin \varphi' \quad (4.2.7)$$

$$s_c = 1 + 0.2 \frac{B}{L} \quad (4.2.8)$$

$$s_\gamma = 1 - 0.3 \frac{B}{L} \quad (4.2.9)$$

where

- B width of the foundation [m]
- L length of the foundation [m]
- $\varphi'$  angle of shearing resistance [ $^\circ$ ]

The effective weight of the soil is calculated using equation (4.2.10). The effective weight under a shallow foundation depends on where the groundwater level is. If the groundwater level rests deeper than the width of the foundation the effective weight is assumed to be the average soil unit weight (Sällfors 2009).

$$\bar{\gamma} = \gamma' + \frac{h_g}{B} \times (\gamma - \gamma') \quad (4.2.10)$$

where

- $\bar{\gamma}$  effective unit weight of the soil [ $\text{kN/m}^3$ ]
- $\gamma'$  effective unit weight of the soil under groundwater level [ $\text{kN/m}^3$ ]
- $h_g$  depth of the groundwater under the foundation [m]
- B width of the foundation [m]

### 4.3 California Bearing Ratio (CBR)

The California Bearing ratio (CBR) has been used since the 1930s to determine the supporting characteristics of soils. CBR is a test method to determine the bearing capacity of the material in the subgrade, sub-base and base layer. CBR is a load test applied on the surface of the soil and is used to determine the pavement design (Mannering et al, 2005). The CBR-value is defined as the load required penetrating the investigated soil compared with a standard soil consisting of well-graded crushed stone. The ratio between these loads is the CBR and it is expressed as a percentage. For example CBR 20 means that it requires 20 percentage of the load compared to the standard material to penetrate the test soil (Mannering et al, 2005).

The standard CBR test is normally conducted on disturbed samples in laboratories but tests can also be performed on undisturbed samples and in-situ (Wright, 2004). The standard equation is presented below (Wright, 2004).

$$CBR \% = \frac{\text{unit load at 2.54 cm penetration}}{\text{unit load required to penetrate the standard}} \times 100 \quad (4.3.1)$$

The standard CBR test compares the required load to penetrate 2.54 cm (1 inch) of the soil sample with the reference load, usually 1000 lb/in<sup>2</sup> (6900 kPa) to penetrate a standard soil sample of crushed rock. (Wright 2004)

According to Mannering et al (2005) there is a relationship between the California bearing ratio and the modulus of subgrade reaction,  $k_0$ . The modulus  $k$  is assumed to be constant under the road structure. The relationship between CBR and the subgrade modulus is presented in Table 4.6 below (Mannering et al, 2005).

Table 4.6 Relationship between CBR and subgrade modulus,  $k_0$  (Mannering et al, 2005)

CBR	Soil type	Subgrade modulus, $k_0$ [MN/m <sup>2</sup> /m]
2	Organic soil	27.145
10	Clay	54.289
25	Sand	78.720
50	Crushed stone- Low	135.724
100	Crushed stone- High	217.158

#### 4.4 Winkler model

The Winkler model is used to analyse the deflection of temporary road mats with an imposed load on different soil types. The theory in this section is derived for beams on a Winkler foundation in two dimensions. The plastic mats described in chapter 3 are assumed to behave like beams in two dimensions and thus this theory is applicable.

The Winkler model is a simple analytical model of an elastic foundation. The model states that if a deflection  $w$  is imposed on the foundation, it resists pressure corresponding to  $k_0w$ , where  $k_0$  is the foundation modulus. In the Winkler model the soil is seen as a foundation that consists of infinite number of springs with a foundation modulus  $k_0$  (Cook, 1999). With this model the soil is assumed to behave linear elastic, as seen in Figure 4.4, which is not completely correct but it gives an adequate estimation of the soil's behaviour compared to measured values (Larsson, 2008).



Figure 4.4 Load applied on a Winkler foundation (Based on Cook, 1999)

It is convenient to use a modulus  $k$  instead of  $k_0$  for calculation of structures with a width  $b$  in contact with the ground (Cook, 1999).

$$p = kw = k_0bw \quad (4.4.1)$$

where

- $p$  pressure [ $\text{N/m}^2$ ]
- $k_0$  foundation modulus [ $\text{N/m}^2/\text{m}$ ]
- $b$  width of beam in contact with ground [ $\text{m}$ ]
- $k$  foundation modulus [ $\text{N/m/m}$ ]

Beam theory on Winkler foundation gives the following equilibrium equations depending on the vertical forces and the resulting moment (Cook, 1999). The relationship between a beam's vertical load and moment on a Winkler foundation is derived from Figure 4.5.

$$\frac{dV}{dx} = -q + kw, \frac{dM}{dx} = V \rightarrow \frac{d^2M}{dx^2} = kw - q \quad (4.4.2)$$

$$M = -EI \frac{d^2w}{dx^2} \quad (4.4.3)$$

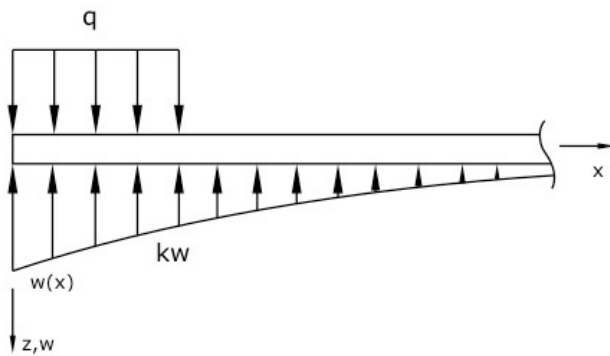


Figure 4.5 Beam with a load  $q$  on a Winkler foundation (Cook, 1999)

By combining the equations above it results in the governing solution for a beam on Winkler foundation.

$$EI \frac{d^4w}{dx^4} + kw = q \quad (4.4.4)$$

From equation (4.4.4) an expression for the deflection can be derived, seen in equation (4.4.6). For the fully derived equation see *Advanced mechanics of materials* (Cook, 1999). To make the function of the deflection contain fewer constants a parameter beta is introduced

$$\beta = \left( \frac{k}{4EI} \right)^{\frac{1}{4}} \quad (4.4.5)$$

where

- $E$  modulus of elasticity [ $\text{N/m}^2$ ]
- $I$  moment of inertia [ $\text{m}^4$ ]

The moment of inertia is calculated as follows

$$I = \frac{b \times h^3}{12} \quad (4.4.6)$$

where

h thickness of the beam [m]

b width of the cross-section [m]

According to Cook the equation for deflection can be written as

$$w(x) = e^{\beta x}(C_1 \sin \beta x + C_2 \cos \beta x) + e^{-\beta x}(C_3 \sin \beta x + C_4 \cos \beta x) \quad (4.4.7)$$

Four different functions are introduced to make the calculation more convenient.

$$\begin{aligned} A_{\beta x} &= e^{-\beta x}(\cos \beta x + \sin \beta x), B_{\beta x} = e^{-\beta x} \sin \beta x \\ C_{\beta x} &= e^{-\beta x}(\cos \beta x - \sin \beta x), D_{\beta x} = e^{-\beta x} \cos \beta x \end{aligned} \quad (4.4.8)$$

These equations can be used to calculate different loading cases for beams on a Winkler foundation. For most cases it is a good approximation to calculate the deflection using an infinite beam with a concentrated load (Cook 1999).

#### 4.4.1 Infinite beam with concentrated load

For a finite beam where  $\beta L > 3$ , the theory for infinite beams can be used according to Cook.

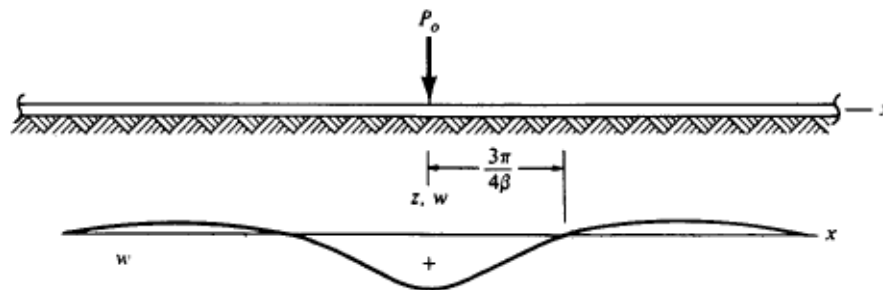


Figure 4.6 Concentrated load on infinite beam and corresponding deflection  $w$ . (Cook, 1999)

On an infinite beam where  $x$  is the distance from the load,  $w(x)$  must approach zero when  $x$  goes to infinity. Then the constants  $C_1$  and  $C_2$  from equation (4.4.7) must be equal to zero as well. What remains in the governing equation is then

$$w(x) = C_3 B_{\beta x} + C_4 D_{\beta x} \quad (4.4.9)$$

To determine the constants C3 and C4 it is necessary to use theory from semi-infinite beams with concentrated end loads. The derived equations for the constants can be seen in *Advanced mechanics of materials*. Finally, this results in the following equation for the deflection (Cook, 1999).

$$w(x) = \frac{\beta P_0}{2k} A_{\beta x} \quad (4.4.10)$$

where

$w(x)$	Deflection at distance x from the load [m]
$P_0$	Centric concentrated load on beam [N]
$\beta$	Beta-factor, see equation (4.4.5) [ $m^{-1}$ ]
$k$	foundation modulus [N/m/m]
$A_{\beta x}$	Function depending on $\beta$ and x, see equation (4.4.8) [-]

The deflection for a beam on a Winkler foundation can be calculated with equation (4.4.10)

## 5 Description of computer software

PLAXIS 2D is a finite element software used for geotechnical analysis' in two dimensions such as deformation and stability calculations of geotechnical structures. Bearing capacity, deflection of plates and settlements is possible to calculate with the software, thus it is used in this thesis as a complement to the calculation made by hand (Plaxis, 2014).

The software is divided into three different programs; input, calculation and output. In the input program the model of the considered scenario and its geometry can be built with different tools such as geometric lines, structural elements and loads. This is modelled in two dimensions, where  $x$  is the horizontal direction and  $y$  is the depth. In the input program it is possible to specify the properties of the soil layer, structural elements and loads (Plaxis, 2014).

In the calculation program the input model can be analysed with different aspects and the results of the analysis are shown in the output program. The results that are presented in the output program can be modified to view deformations, stresses and also to create charts.

It is possible to model in two different ways in PLAXIS 2D; plain strain model or axisymmetric model. The plain strain model is ideal to use for continuous structures with uniform cross section in the out of the plane direction, as seen in Figure 5.1 below.

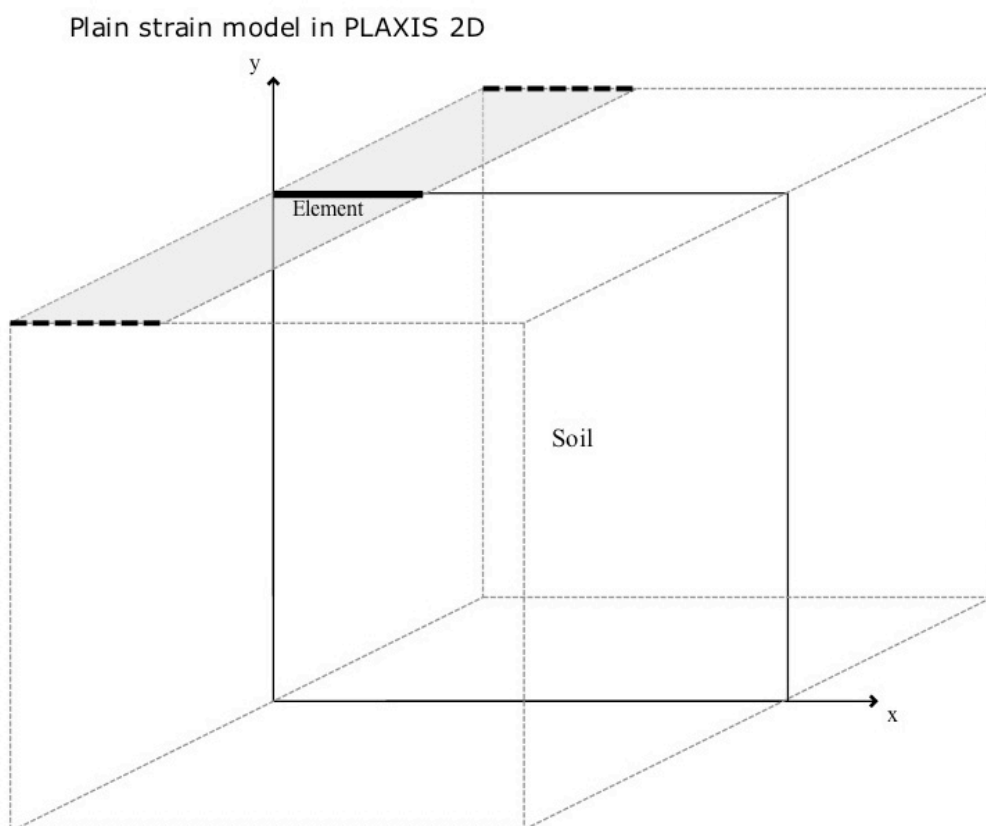


Figure 5.1 A plain strain model in PLAXIS 2D.

The axisymmetric model assumes a structure that is rotated around the y-axis with a constant radial cross section. This model is a good estimation to use for circular footings and when loads are acting parallel to the symmetry line. The coordinates along the x-axis represent the radius and y-axis the symmetry line. Figure 5.2 illustrates how the real circular model in 3D is modelled in PLAXIS 2D using an axisymmetric model (Plaxis, 2014).

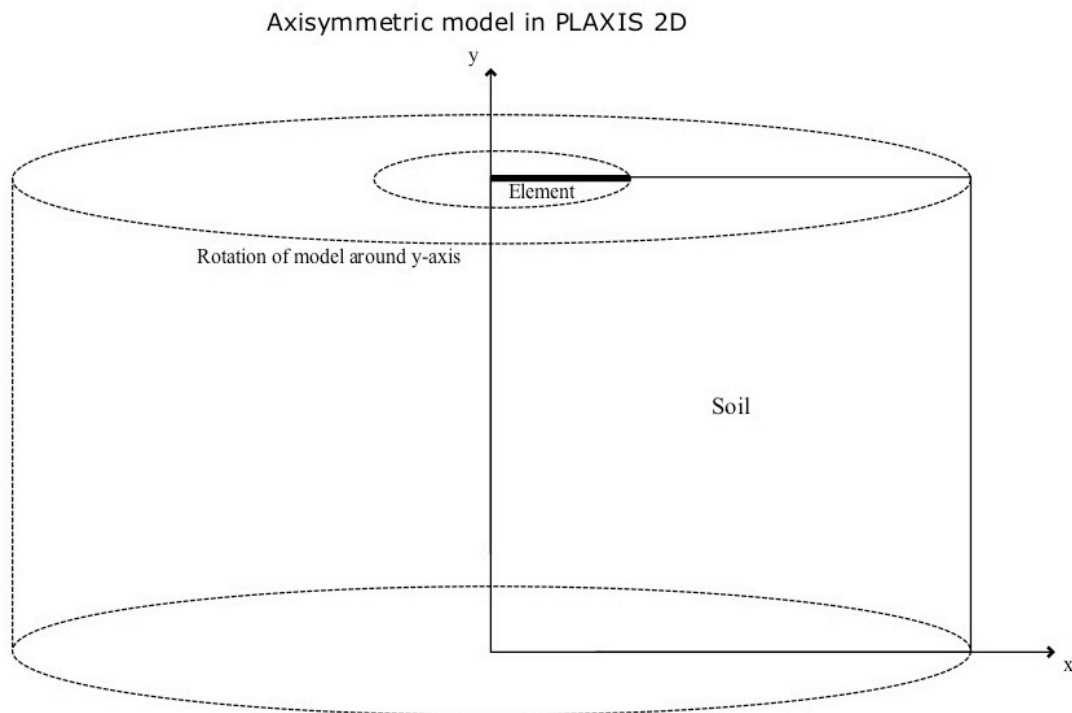


Figure 5.2 An axisymmetric model in PLAXIS 2D

PLAXIS 2D also has a function to automatically generate a mesh for the model. This mesh is in form of unstructured triangular finite elements and is necessary to be able to calculate. The mesh will automatically be finer closer to the structure and the loads to make the calculations more accurate. There are two types of elements available in PLAXIS 2D; a quadratic six-node and a fourth order polynomial element with 15 nodes (Plaxis, 2014).

PLAXIS 2D has several soil models available for the user to use in the modelling. The Mohr-Coulomb model is one of the models, which assumes the soil to be linear elastic perfectly plastic. The model involves five input parameters that the user can modify;

- E modulus of elasticity
- $\nu$  Poisson's ratio
- $\phi$  angle of shearing resistance
- $c, s_u$  soil plasticity, cohesion or undrained shear strength
- $\psi$  angle of dilatancy

## 6 Case study

In the case study the road mats' behaviour for different soils and loading positions is investigated. The theory presented in earlier chapters is applied on the TuffTrak road mat. The bearing capacity is calculated with the general bearing capacity equation to determine the allowable bearing pressure from the mat. The deflection of the mat on different soils is analysed with the Winkler model. The Winkler model presents the instantaneous deflection that occurs when a tire load is applied at the centre of the mat. Finally the cases are analysed in PLAXIS 2D to determine the performance of the mat, which includes both bearing capacity and deflection. The results from the PLAXIS 2D are compared to the hand-calculations to see if the models are correlated.

### 6.1 Description of cases

Three cases are chosen to represent common ground conditions in Sweden. The cases are seen in Figure 6.1 with respective values in Table 6.1. Strength parameters in the soil vary from site to site, consequently it is difficult to analyse all possible conditions. Thus typical values are chosen to be able to estimate feasible scenarios of deflection and failure of the temporary road.

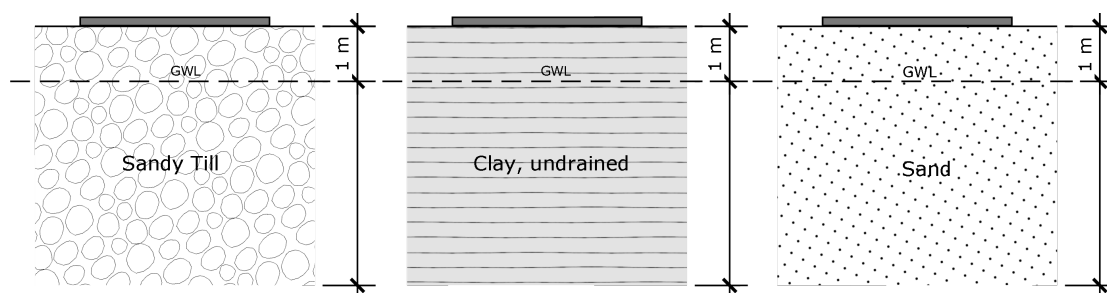


Figure 6.1 The three cases of consideration in the case study.

Table 6.1. Chosen values for the different cases

Description	Parameter	Sandy Till	Clay, undrained	Sand
Angle of shearing resistance	$\phi'$ [ $^{\circ}$ ]	42	0	32
Soil unit weight, saturated	$\gamma_{\text{sat}}$ [ $\text{kN/m}^3$ ]	22	17	20
Effective soil weight under GWL	$\gamma'$ [ $\text{kN/m}^3$ ]	12	7	10
Cohesion, undrained shear strength	$c, c_u$ [ $\text{kPa}$ ]	0	50	0
Modulus of elasticity	$E$ [ $\text{MN/m}^2$ ]	70	20	40
Foundation modulus	$k_0$ [ $\text{MN/m}^3$ ]	135.7	54.3	78.7
Poisson's ratio	$\nu$ [-]	0.2	0.4	0.3

For the bearing capacity calculations the parameters of consideration are; the angle of shearing resistance, the soil unit weight and the undrained shear strength. The Winkler model considers the mat's properties and the foundation modulus  $k$ , which the calculated deflections are based on. Elastic modulus and Poisson's ratio are used for the finite element calculations in PLAXIS 2D.

Common condition for the three cases is that the groundwater level (GWL) is assumed to be one meter below the surface as seen in Figure 6.1. How the GWL affect the result is also analysed in the parametric study. The groundwater level determines the effective weight of the soil and therefore it is important to investigate other levels of ground water to see how it affects the bearing capacity.

Sandy Till is one of the most common types of tills and thus chosen as a case. The sandy till is a non-cohesive soil and consequently the cohesion is set to zero. In the parametric analysis the angle of shearing resistance is varied to see how it affects the result. The foundation modulus for the sandy till is assumed to be the same as for "crushed rock low" described in chapter 4.3. This is an assumption that may underestimate the deflection in the Winkler model.

The case of clay only considers the undrained state due to the short time of loading and that the load is temporary. It is assumed that the loading will be relatively short term, thus the clay will not consolidate and change state to drained condition. This is further described in chapter 4.1.

All of the cases are modelled as one homogenous layer with the same material properties along the depth. The reason for this is because it makes the calculations and the parametric analysis comparable.

### 6.1.1 Special case

A special case is also analysed in PLAXIS 2D. This is made as a complement to the other cases to simulate a scenario with more than one layer. The case analyses how the mat acts on soft topsoil with an underlying dry crust followed by another layer of clay. Two calculations are made for this case; first with all considered layers and second without the topsoil. With these two calculations one can see how the mat distributes a load on a soft soil and also how the dry crust mobilise the stress. The parameters for the layers are seen in Table 6.2.

*Table 6.2 Parameters and values used in the special case*

Layer	Depth	$c_u$ [kPa]	E [MPa]
Topsoil	20 cm	5	5
Dry crust	30 cm	50	50
Clay	>5 m	25	20

## 6.2 Loads

The considered load is where the axle pressure is assumed to be greatest. This is normally at the rear axle on the trailer where duals are used. How the load is placed on the mat for the bearing capacity calculation is seen in Figure 6.2.

Assumptions:

- 2 meters track width (centre-to-centre distance between duals).
- Axle load of 17,000 kg
- The axle load is spread with 55 % and 45 % on the duals.
- The mats are placed in rows of two with the shortest side in the driving direction.
- The tires are placed equally on each mat, one meter from the edge.
- The load is acting on one standalone mat without connection.

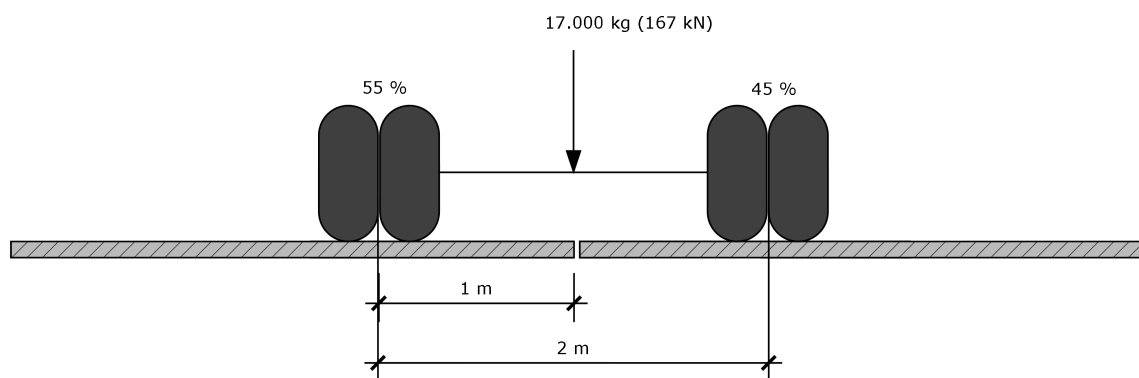


Figure 6.2 Dual tires on the plastic road mat.

The pressure that the plate acts on the ground varies with the position of the tire load, which is related to the effective area. The effective area is greatest when the load is applied at the middle and decreases as the load reaches the edges. Thus the plate pressure is calculated for different positions along the mat, see Figure 6.3. For the calculations of bearing capacity and deflection only one mat and one dual tire are considered. The calculated tire load is

$$\text{Tire load} = 55 \% \text{ of } 17,000 \text{ kg} \times 9.81 = 91.7 \text{ kN}$$

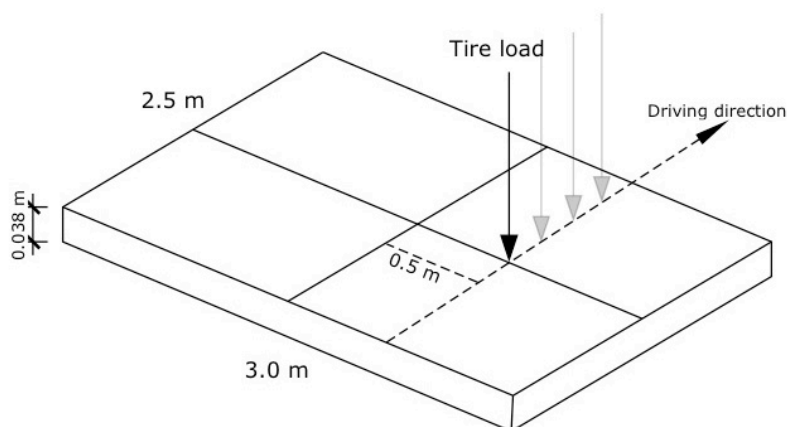


Figure 6.3 The different positions on the mat where the load is applied.

The load is constantly 0.5 m from the centre and changes position from 0 to 1.1 m from the centre line. The 0.5 meter distance from the centre represents the position of one of the duals while the other one is assumed to be positioned parallel at the adjacent mat. The reason for choosing 1.1 m as the furthest distance from the centre is due to the fact that the tire length is assumed to be 30 cm and hence 15 cm from the edge is the most critical point where one mat has to support the entire load.

The presented plate pressure is compared to the calculated bearing capacity for different soils. As seen in Figure 6.4 the plate pressure increases when the load is placed further to the edge of the mat. The maximum pressure at the edge is 153 kPa, thus this value is compared to the bearing capacity of the different cases.

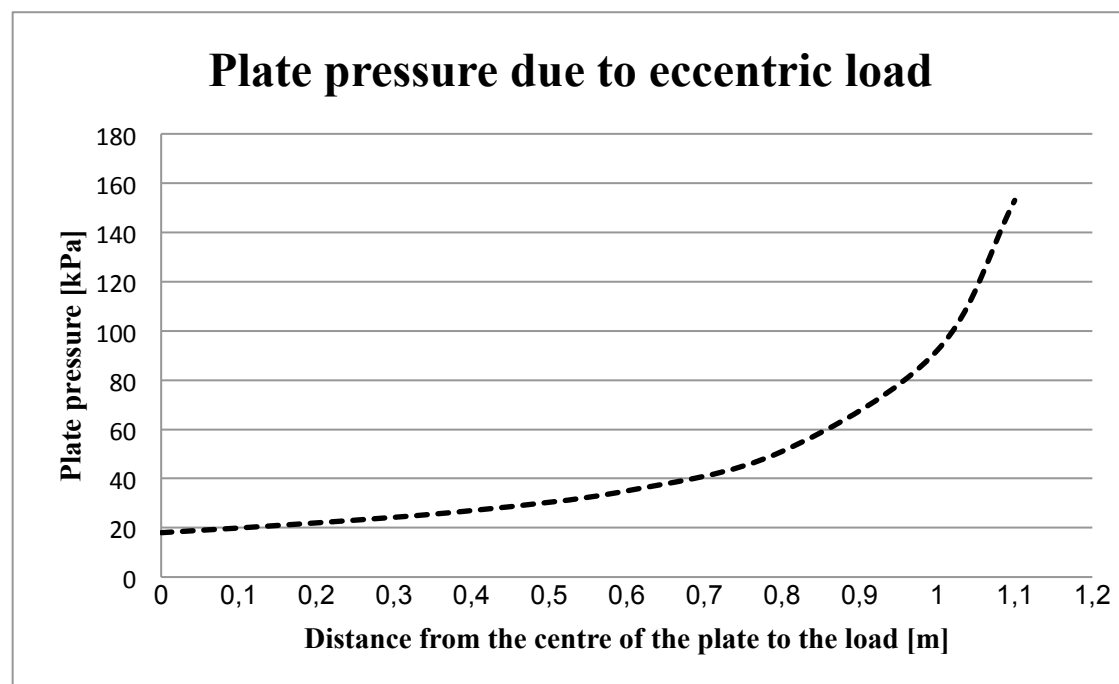


Figure 6.4 Plate pressure at different positions along the mat.

### 6.3 Bearing capacity

The bearing capacity for the different cases is calculated using equation (4.2.2). The bearing capacity is compared to the calculated plate pressure. If the value of the bearing capacity exceeds the plate pressure it can bear the load, otherwise there is a need of reinforcements under the mat. For the three cases it is assumed that the ground is flat, thus the inclination factor is removed from the equation. The mat will be positioned directly on the ground and therefore there will not be any surcharge load. The assumptions reduce the bearing capacity equation to

$$q_f = cN_c s_c + \frac{1}{2} \gamma' B_{ef} N_\gamma s_\gamma$$

For the case of the undrained clay the undrained shear strength,  $c_u$ , is valid while the angle of shearing resistance is zero, thus the value of  $N_c$  and  $N_\gamma$  is set to 5.14 respectively zero according to (Sällfors, 2009). For the case of the sandy till and the sand the cohesion is zero while the angle of shearing resistance depends on the material investigated. The cases are for one specific situation but a parametric study is

conducted for each case to determine which parameters that are the most sensitive for the results.

The bearing capacity is calculated for one scenario where the effective width and length is constant. The effective width and length of the mat is calculated using equation (4.2.3) and is assumed to be the same for all of the three cases. The distance from the centre of the mat to the load is assumed to be 0.5 meter, which result in an effective width and length of:

$$B_{ef} = B - 2e_B \rightarrow B_{ef} = 3 - 2 \times 0.5 = 2 \text{ m}$$

$$L_{ef} = L = 2.5 \text{ m}$$

### 6.3.1 Sandy Till

In this specific case the groundwater is assumed to be one meter below the foundation and the effective weight can be calculated using equation (4.2.10). The angle of shearing resistance is set to  $42^\circ$  while the effective weight depends on where the groundwater level is set. The effective weight is calculated as follows

$$\bar{\gamma} = \gamma' + \frac{h_g}{B} \times (\gamma_{sat} - \gamma') = 12 + \frac{1}{3} \times (22 - 12) = 15.33 \text{ kN/m}^3$$

Since there is no cohesion and no surcharge load the general bearing capacity is reduced to the following state

$$q_f = \frac{1}{2} \gamma_m B_{ef} N_\gamma s_\gamma$$

The shape factor  $s_\gamma$  and  $N_\gamma$  are calculated using the equations (4.2.6) respectively (4.2.4)

$$s_\gamma = 1 - 0.3 \frac{B_{ef}}{L_{ef}} = 1 - 0.3 \frac{2}{2.5} = 0.76$$

$$N_\gamma = 151.94$$

The bearing capacity for this case is calculated

$$q_f = \frac{1}{2} \bar{\gamma} B_{ef} N_\gamma s_\gamma = \frac{1}{2} \times 16 \times 2 \times 151.94 \times 0.76 = 1771 \text{ kPa}$$

Comparing the results from the bearing capacity calculation with the plate pressure determines if the soil will tolerate the pressure. If the ratio is less than one it means that failure will occur.

$$\frac{q_f}{q_{load}} = \frac{1771 \text{ kPa}}{153 \text{ kPa}} = 11.58$$

The result from the equation above shows that the bearing capacity of the soil is 11.58 times higher than the pressure of the plate. This means that it is safe to use the mats in the conditions presented in this case.

### 6.3.2 Undrained Clay

Clay is a common soil in Sweden and for that reason it is important to have it as a case. This case is for undrained clay because the load and construction are assumed to

be temporary and relatively short term. The undrained shear strength is set to 50 kPa and the angle of shearing resistance is 0° as (Sällfors, 2009) suggests.

To determine the bearing capacity for the undrained clay it is required to calculate the shape factors. Due to the fact that the angle of shearing resistance is set to 0°, shape factor  $s_y$  will not contribute to the bearing capacity and therefore only  $s_c$  is considered.

$$s_c = 1 + 0.2 \frac{B_{ef}}{L_{ef}} = 1 + 0.2 \left( \frac{2}{2.5} \right) = 1.16$$

According to (Sällfors, 2009) the value for  $N_c$  is 5.14 when the angle of shearing resistance is zero. The bearing capacity for undrained clay results in

$$q_f = c_u N_c s_c = 50 \times 5.14 \times 1.16 = 298 \text{ kPa}$$

Comparing this with the pressure from the plate gives a safety factor of

$$\frac{q_f}{q_{load}} = \frac{298 \text{ kPa}}{153 \text{ kPa}} = 1.95$$

The safety factor for the case of undrained clay is 1.95, which means that the soil is able to handle the load.

### 6.3.3 Sand

To calculate the bearing capacity for the sand case it is required to determine the properties for the sand. In the case of consideration the angle of shearing resistance is set to 32° while the cohesion is zero. In this specific case the groundwater is assumed to be one meter below the foundation and the effective weight of the soil is calculated with equation (4.2.10)

$$\bar{\gamma} = \gamma' + \frac{h_g}{B} \times (\gamma_{sat} - \gamma') = 10 + \frac{1}{3} \times (20 - 10) = 13.33 \text{ kN/m}^3$$

Since there is no cohesion and no surcharge load, the general bearing capacity is reduced to the following state

$$q_f = \frac{1}{2} \bar{\gamma} B_{ef} N_\gamma s_\gamma$$

$s_\gamma$  and  $N_\gamma$  are calculated using equation (4.2.9) respectively (4.2.6)

$$s_\gamma = 1 - 0.3 \frac{B}{L} = 1 - 0.3 \frac{2}{2.5} = 0.76$$

$$N_\gamma = 27.72$$

The calculated bearing capacity for the sand case is

$$q_f = \frac{1}{2} \bar{\gamma} B_{ef} N_\gamma s_\gamma = \frac{1}{2} \times 13.33 \times 2 \times 27.72 \times 0.76 = 281 \text{ kPa}$$

Comparing the bearing capacity with the pressure from the plate gives the safety factor

$$\frac{q_f}{q_{load}} = \frac{281 \text{ kPa}}{153 \text{ kPa}} = 1.84$$

## 6.4 Deflection of the plate using Winkler model

The Winkler model is used to determine the deflection of the mat on different soils. The deflection obtained in the Winkler model is compared to the deflection calculated in PLAXIS. The derived equation for the deflection of a Winkler foundation can be seen in chapter 4.4. The deflection  $w(x)$  is calculated using the equation below where the  $k$  value is depended on the investigated soil while the  $A_{\beta x}$  factor is depended on the distance from the load. For each case the point load is assumed to be 92 kN and placed at the centre of the foundation.

$$w(x) = \frac{\beta P_0}{2k} A_{\beta x}$$

The investigated TuffTrak mat is 3 times 2.5 meters and is assumed to behave like an infinite beam on Winkler foundation. The analysis is in 2-dimensions and therefore the  $k_0$ -value needs to be multiplied with the length in contact with the ground to get the right foundation modulus, see equation (4.4.1). For this analysis it is assumed that the length in contact with the soil is one meter and hence the  $k$ -factor is calculated as

$$k = k_0 \times b = k_0 \times 1$$

The  $k_0$  values for different soils can be found in chapter 4.4. It is assumed that the  $k_0$  value for the sandy till is equal to the value for “crushed stone low”, which may underestimate the result of the deflection. On the other hand the deflection may be overestimated if the  $k_0$  is the same as for sand.

The moment of inertia is calculated using 4.4.6 and the modulus of elasticity for the mat is 900MPa

$$I = \frac{b \times h^3}{12} = \frac{2.5 \times 0.038^3}{12} = 1.143 \times 10^{-5} \text{ m}^4$$

The  $\beta$ -factor needs to be calculated for each specific case due to the fact that it is dependent on the foundation modulus,  $k$ . The  $\beta$ -factor is calculated using 4.4.5 and the calculated values are presented in Table 6.2 below.

$$\beta = \left( \frac{k}{4EI} \right)^{\frac{1}{4}}$$

Table 6.2  $k$  and  $\beta$  values for the different cases

Parameter	Unit	Sandy Till	Clay, undrained	Sand
$k$	[MN/m/m]	135.7	54.3	78.7
$\beta$	[m <sup>-1</sup> ]	6.03	6.61	7.58

To calculate the deflection at different points on the mat it is required to use the  $A_{\beta x}$ -function, which depends on the  $\beta$  factor and the distance,  $x$ , from the load.

$$A_{\beta x} = e^{-\beta x} (\cos \beta x + \sin \beta x)$$

The TuffTrak mat is 3 meters wide and therefore the distance that needs to be investigated is from the centre of the mat and 1.5 meter to the edge.

By using these equations together it results in the deflections shown in Figure 6.5 for the chosen cases.

The results show that the deflection for the clay is greatest and correspond to around 5 mm. The deflection for the sand case is around 4 mm while for the sandy till case it is about 2.5 mm.

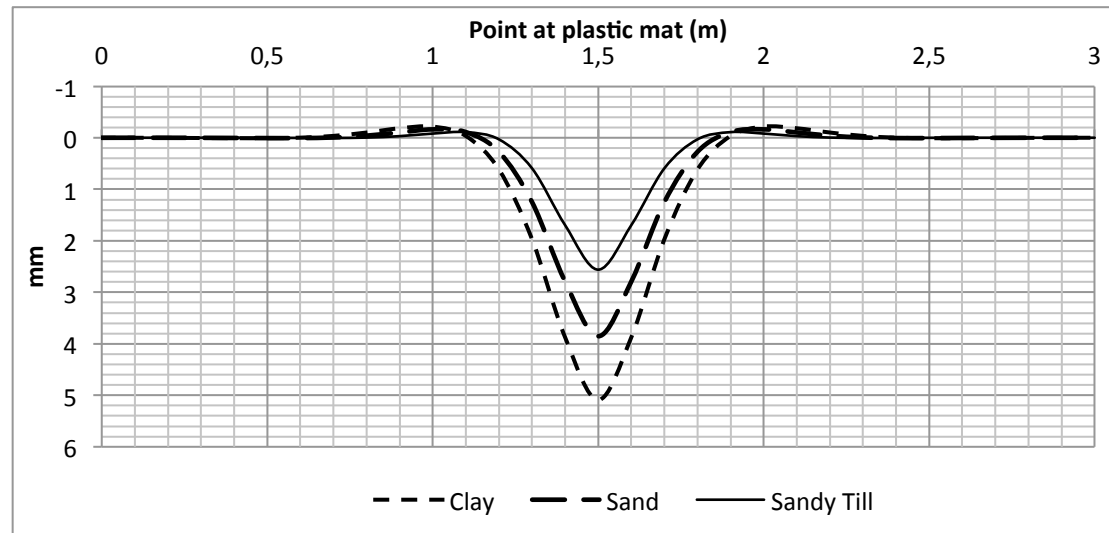


Figure 6.5 The calculated deflection for clay, sand and sandy till on a Winkler foundation.

Maximum allowable deflection of the road depends of how sensitive the transports are to uneven surfaces. Requirements from Vestas are that the lateral gradient of the road shall not exceed  $2^\circ$ . When using temporary roads on undisturbed soil, there is no guarantee that the surface will deflect equally under the two tires. The maximum allowable difference in deflection for a 2 meter wide axle to tilt  $2^\circ$  is calculated as follows

$$\sin(2^\circ) = \frac{x}{2000} \rightarrow x = 70 \text{ mm}$$

This means that if the mat deflects more than 70 mm under one side of the transport and the other side does not deflect at all, the axle will tilt more than  $2^\circ$  which is not recommended by Vestas.

## 6.5 PLAXIS 2D

The analysis in PLAXIS 2D is conducted with an axisymmetric model. This means that the model is symmetric around the y-axis and hence the model will be circular around the y-axis. The axisymmetric model is used to determine how a single mat reacts to a given load. The plain strain model is not used because the mat would be continuous in one direction and therefore the results would not be accurate for a single mat.

The parameters used for the soil models in PLAXIS are presented in Table 6.1. For the cases of sand and sandy till the cohesion is set to 1 kPa due to numerical limitations in the software. The clay is modelled as a rectangle with sides of 5 and 4 meters, where the later represents the depth. The sand and sandy till are modelled as a

square with sides of 20 meters. GWL is set to one meter beneath the surface as in previous calculations. Due to the axisymmetric model the plate is modelled as a circular footing. The circular footing represents the effective area of the plate, which varies with the load's position.

### 6.5.1 Distributed load

The axial load is transferred to the tires and therefore the contact area for the tires needs to be calculated to determine the pressure on the plate due to the load. For the dual tires the contact area is determined using equation (2.1.5) in chapter 2.

It is assumed that the spacing between duals,  $S_d$  is 0.3 meters, the load on the tires is 92kN and the tire pressure,  $q$  is 800 kPa. These are values that are typical for trailers as mentioned in Chapter 2. With these assumptions it is possible to calculate the contact area for the tires using equation (2.1.5).

$$\pi a^2 = \frac{0.8521P_d}{q} + S_d \sqrt{\frac{P_d}{0.5227q}} = \frac{0.8521 \times 92}{800} + 0.3 \sqrt{\frac{92}{0.5227 \times 800}} = 0.239 \text{ m}^2$$

To determine the pressure that is transferred to the mat, the load is divided with the area calculated above.

$$\frac{P_d}{\pi a^2} = \frac{92}{0.239} = 385 \text{ kPa}$$

From equation (2.1.5) it is possible to calculate the radius,  $a$ , for the circular area.

$$a = \sqrt{\frac{0.239}{\pi}} = 0.2758 \text{ m}$$

The radius is used in the axisymmetric model in PLAXIS 2D to analyse if the soil can handle the distributed load from the tire.

### 6.5.2 Effective area

The effective area of the plate affects the amount of pressure that is transmitted to the soil and hence its ability to handle the loads. Depending on where the load is applied on the mat the effective area varies and so does the bearing capacity of the soil. Therefore it is important to model different cases where the load is applied at different points on the mat.

Due to the axisymmetric model the effective area of the mat is represented by a circular footing, which is assumed to be similar to how the area would be in reality. For the analysis in PLAXIS 2D three different areas with specific radii is considered:

- 1.5 meters, which represents a tire at the centre of the mat.
- 0.5 meters, which represents an edge load.
- 0.34 meter, which represents a corner load.

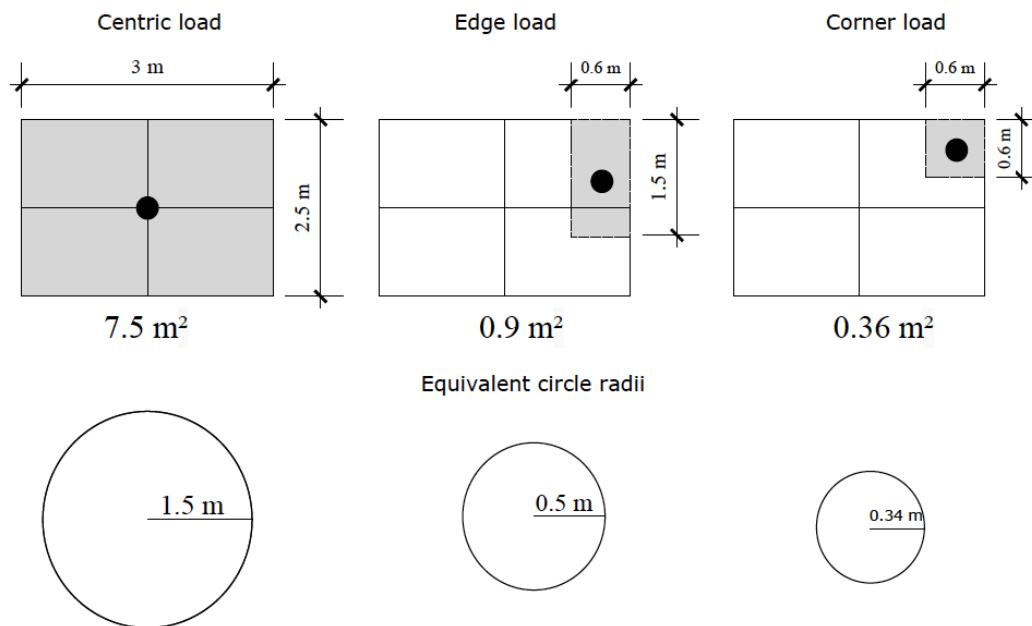


Figure 6.6 Effective area and respective radii used in PLAXIS

Figure 6.6 above illustrates the tire position on the mat and the resulting effective area. The effective rectangular area is transformed to an equivalent circle with radius used in PLAXIS 2D to model the mat. The loading cases are performed on the soils described in Table 6.1 and thus the same parameters are used as in previous calculations.

### 6.5.3 Sandy Till

The first load case represents a tire in the middle of the mat. The effective area is in this case the whole mat. According to the calculations the maximum deflection is 4.5 millimetres (Figure 6.7) and the soil is able to withstand the pressure from the load. The parameters used for the case of sandy till are presented in Table 6.1.

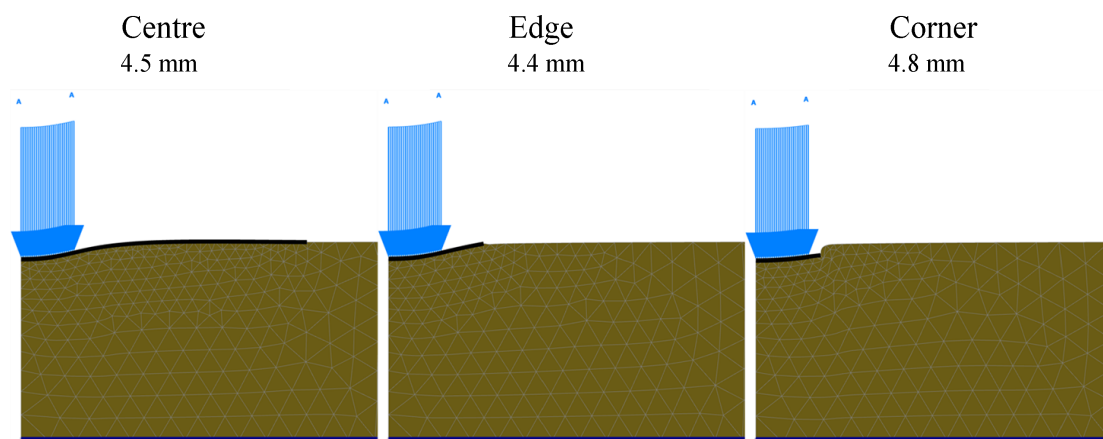


Figure 6.7 The deformation of the sandy till for three loading cases scaled up 20 times.

The maximum deflection at the edge is calculated to be 4.4 millimetres. The soil handles the pressure from the plate and no failure occurs. In the third case the load is

applied at the corner of the mat, which gives a maximum deflection of 4.8 millimetres. According to the calculations, the sandy till should be able to withstand the load for all scenarios.

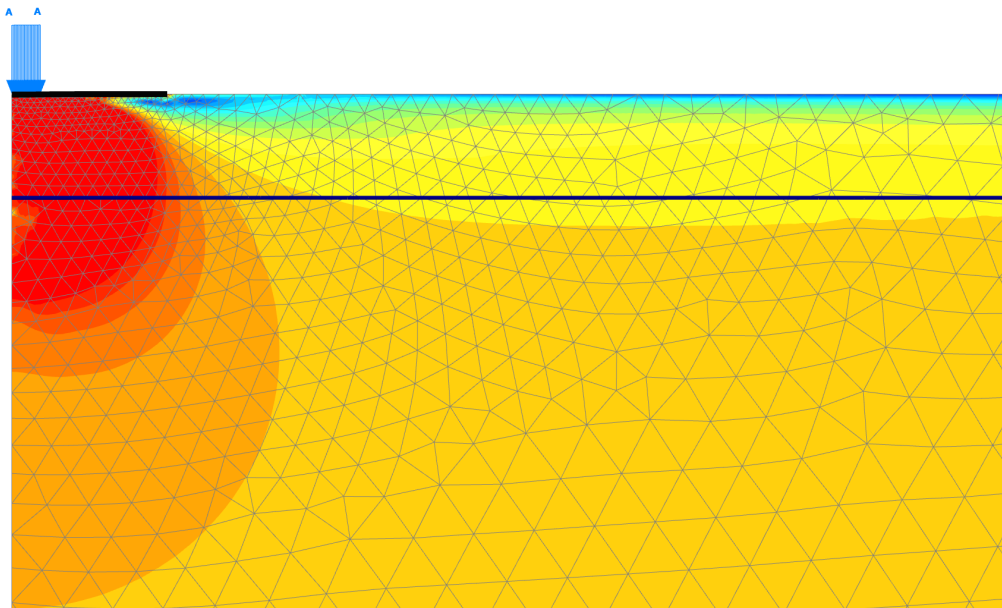


Figure 6.8 The relative shear stress for the load applied at the centre of the mat, where the area directly under the mat has the greatest stress.

Figure 6.8 shows the relative shear stress for the case of sandy till. The relative shear stress is the ratio between the mobilised shear stress and the maximum shear strength. When the ratio for the relative stress is one it means the soil plasticise. Thus the deformation shown in Figure 6.5 is partly a permanent plastic deformation. The area directly beneath the mat shows the greatest stress and it is mainly where the deformation occurs.

#### 6.5.4 Clay undrained

The parameters used for the undrained clay are presented in Table 6.1. The load is applied at the centre, the edge and at the corner of the mat. This approach is used to see how different loading positions affect the deflection and the bearing capacity of the soil.

When the load is acting on the centre of the mat it results in a maximum deflection of 7.5 millimetres for clay, see Figure 6.9.

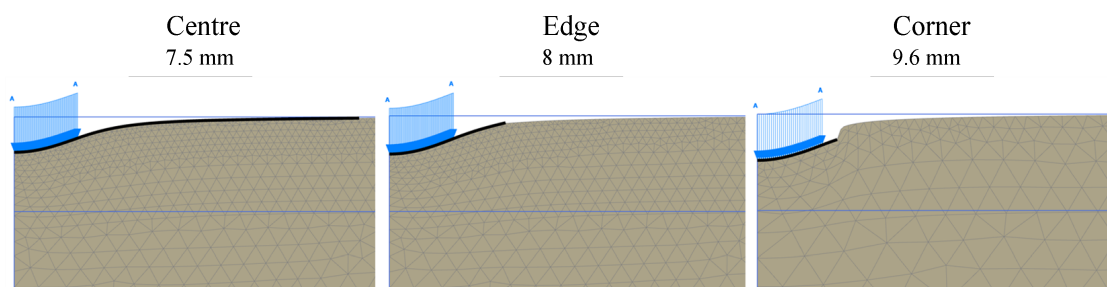


Figure 6.9 The deformation of the clay for three loading cases scaled up 20 times.

The scenario where the load is applied at the edge results in a maximum deflection of 8 millimetres. The corner load results in a maximum deflection of 9.6 millimetres and as for the sandy till no failure occurs according to the calculations.

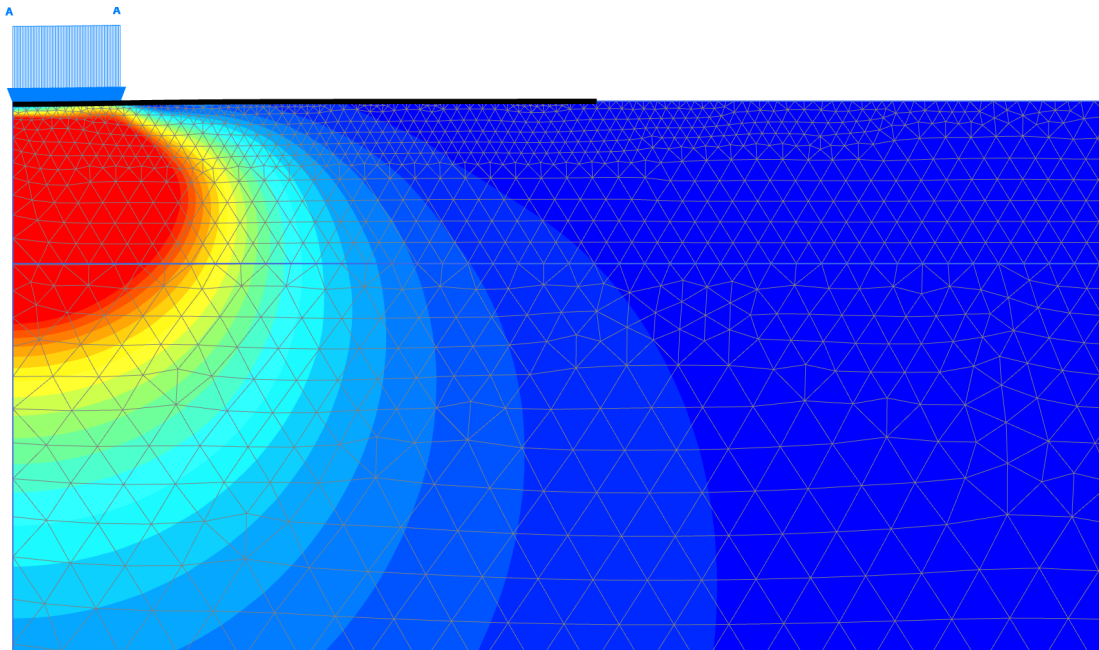


Figure 6.10 The relative shear stress of the undrained clay where the load is applied at the centre. The greatest stress is mobilised directly under the load.

Figure 6.10 shows the relative shear stress for the clay when the load is applied at the centre of the mat. The stress is greatest under the load where the soil partly plasticises and a permanent deformation occurs.

### 6.5.5 Sand

The calculations for the sand case are basically the same as for clay and sandy till, but with different parameters. The maximum deflection of the centre load is 9.2 millimetres and 9.9 for the edge loading case.

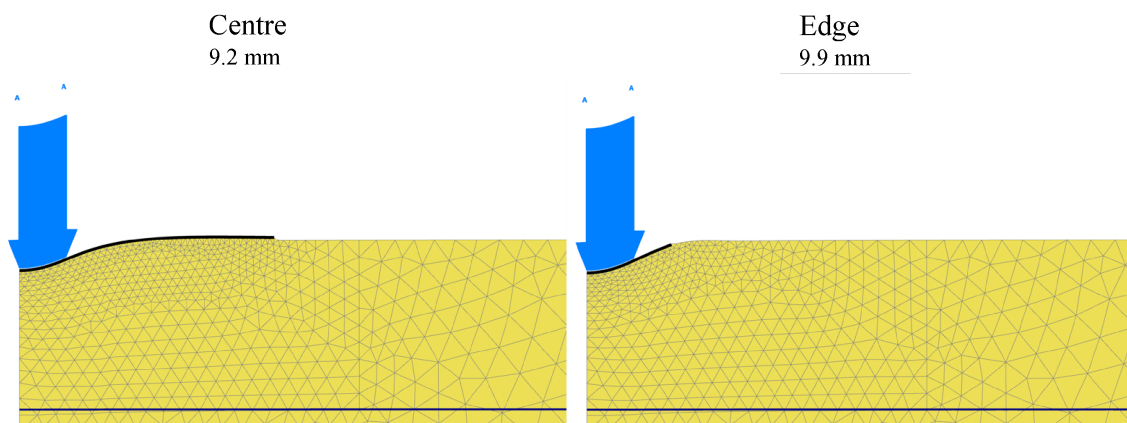
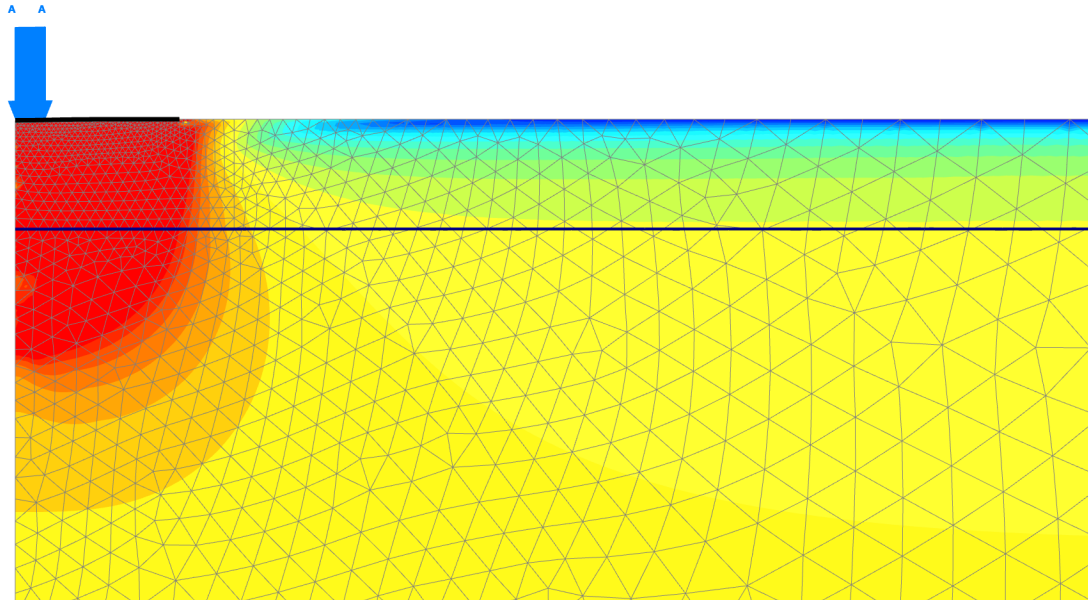


Figure 6.11 The deformation of the sand for centre and edge loading (scaled up 20 times).

The deformations in Figure 6.11 are only presenting centre and edge load because of a failure at the corner load. This happens when too many plastic points occur during the loading stage, thus the iteration process will stop and the software refers to a failure. The reason for not presenting the corner case is due to the fact that the calculations were not fully performed so the resulting deflection does not reflect reality.



*Figure 6.12 The relative shear stress of the sand where the load is applied at the centre. The dark contours under the mat indicate great stress.*

The relative shear stress in Figure 6.12 indicates that plastic deformation occurs under the mat resulting in a permanent deformation.

## **6.6 Special case**

In this chapter two special cases are presented to simulate how the mat behaves when more soil layers are considered. For full description of the case and given soil layer see chapter 6.1. The calculations are made in PLAXIS 2D with the same load as in previous cases, a distributed load of 385 kPa over an area that represents one dual tire. The load is placed in the middle of the mat, which means that the radius of the mat element in PLAXIS 2D is 1.5 meter.

The first case determines how the deformation and stress is spread through clayey soft topsoil to an underlying dry crust. The top layer is 20 cm deep with undrained shear strength of 5 kPa, which is classed as very low strength.

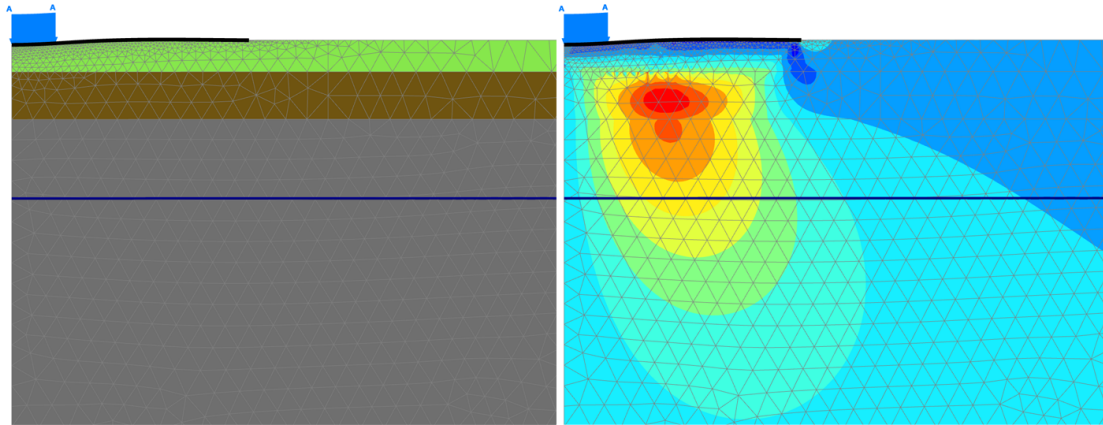


Figure 6.13 The deformation and Cartesian shear stress for the case of 20 cm soft soil and 30 cm dry crust below.

The calculated deflection is 29.9 mm and most of the deflection occurs in the topsoil. The stress is transmitted through the top layer to the dry crust. It is the dry crust that mobilises most of the stresses, as seen in Figure 6.13. The maximum stress corresponds to 15 kPa. When unloading, the deformation is inverted by 15 mm and when loading again it deflects to approximate 30 mm. The deflection obtained is both elastic and plastic. The plastic deformation is permanent and remains during unloading, while the elastic deformation flex back.

The second case is similar to the first case except that the topsoil is removed. The reason for this is to analyse how the dry crust mobilises the stress from the load and also to see the differences in the stress distribution from the mat above a soft layer versus a hard layer.

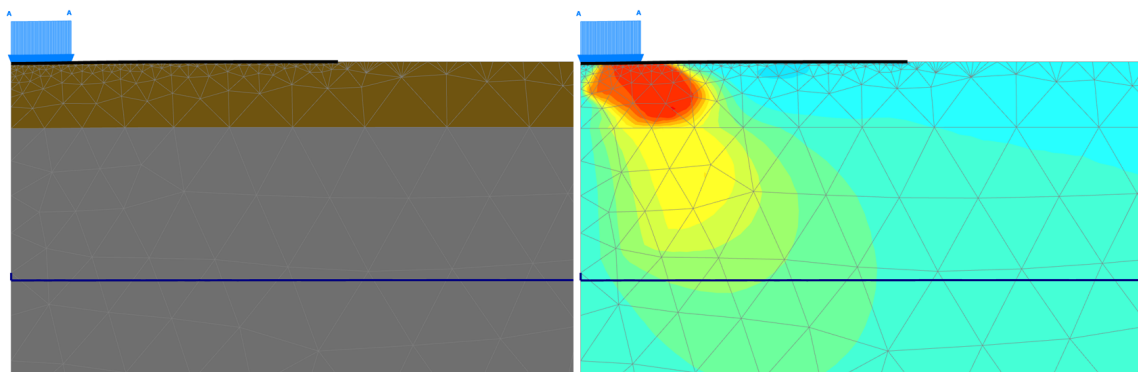


Figure 6.14 The deformation and Cartesian shear stress for the case of 30 cm dry crust on a layer of clay.

The maximum deflection for this case is 8.2 mm and as Figure 6.14 shows the most of the stress is distributed in the dry crust. The maximum stress is 50 kPa directly under the mat. Notice in Figure 6.14 how the stress is mobilised directly under the tire, compared to Figure 6.13, where the stress is evenly distributed.

## 7 Analysis

The analysis is performed to evaluate the results for the bearing capacity and the deflection. The analysis is conducted with a parametric study of the bearing capacity and the PLAXIS 2D calculations. A comparison between the results from PLAXIS 2D and the hand-calculations is then performed to see if correlation exists between the models.

### 7.1 Parametric analysis

The parametric analysis is performed for both the general bearing capacity equation and for the calculations in PLAXIS 2D to determine how different parameters affect the results. The calculations are based on different angle of shearing resistance for the sandy till and the sand case, while the calculations of the clay are based on different values of undrained shear strength.

#### 7.1.1 Bearing capacity

The bearing capacity of the soil is calculated using the general bearing capacity equation presented in chapter 4. To determine which parameters that are the most sensitive to the result a parametric analysis is performed. Three cases for the groundwater are evaluated; one for groundwater at ground level, one for groundwater level 1 m under the foundation and one for the groundwater level at great depth under the foundation. The groundwater level determines the effective weight of the soil and the weight is calculated using equation (4.2.10).

In each Figure the maximum plate pressure of 153 kPa is presented as a horizontal dotted line. When the bearing capacity exceeds this line the soil is able to bear the load.

The angle of shearing resistance for the sandy till and the sand is varied between the values presented in Table 4.2 in chapter 4. For the case of the undrained clay, the undrained shear strength,  $c_u$  is changed between the values presented in Table 4.3. The values that are investigated are summarised in Table 7.1.

Table 7.1 Values varied in the parametric analysis

Soil	Angle of shearing resistance, $\phi$ [°]	Undrained shear strength, $c_u$ [kPa]	GWL
Sandy Till	42-45	-	Ground level - 1 meter below - Great depth
Sand	28-35	-	
Clay	-	5-300	

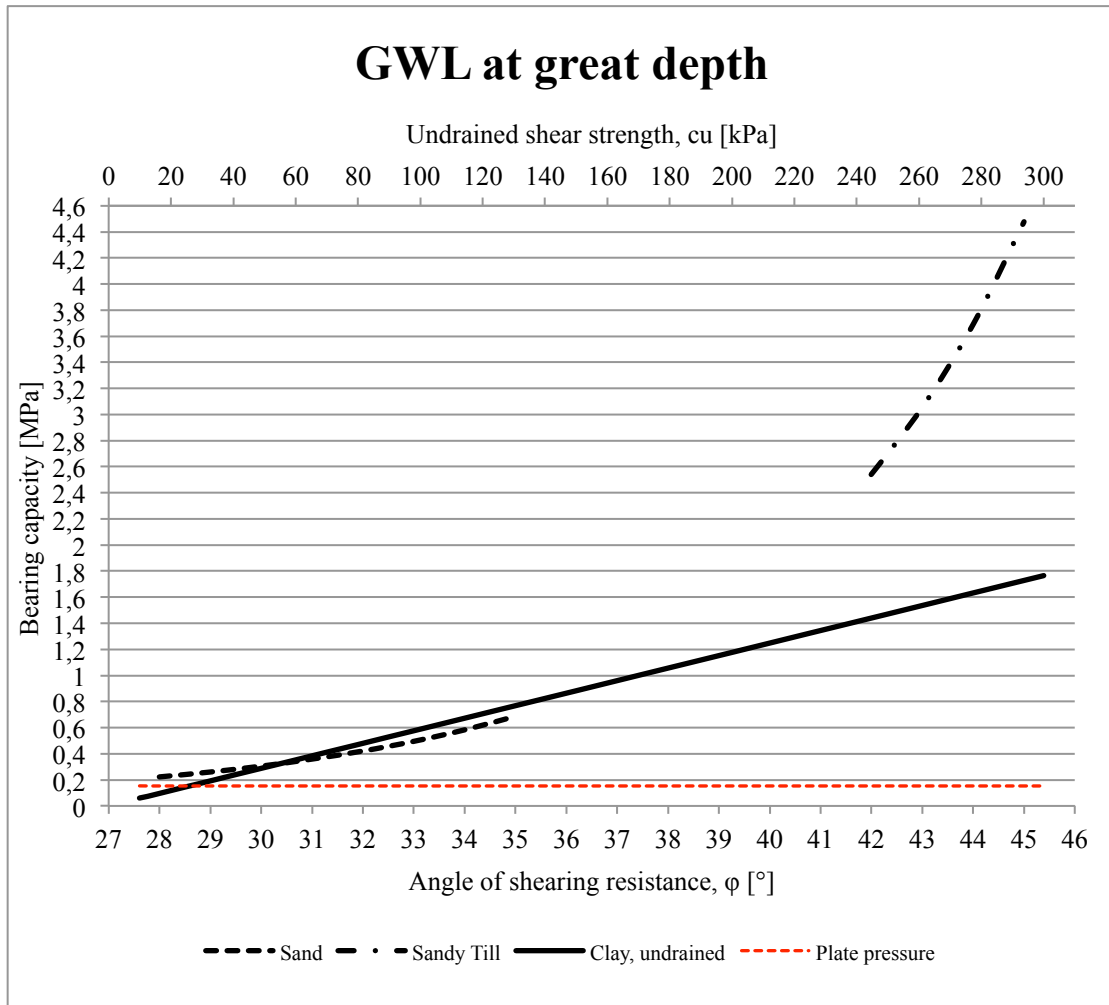


Figure 7.1 Parametric analyses of the bearing capacity for different soil parameters (GWL at great depth).

In Figure 7.1 the bearing capacity for the three soils is presented. The bearing capacity is calculated for groundwater at a great depth below the foundation. As Figure 7.1 shows the most critical soils are clay and sand where the bearing capacity for some of the investigated parameters lays under the pressure from the plate. When the angle of shearing resistance is  $28^\circ$  for the sand it corresponds to a bearing capacity of 222 kPa. This means that with an angle of  $28^\circ$  the sand should be able to handle the load.

The undrained shear strength of the clay needs to exceed 25 kPa to handle the considered load. Otherwise the bearing capacity will be too low compared to the maximum plate pressure and a failure will occur.

The bearing capacity for the sandy till case is much greater than the pressure of the plate and it is fairly safe to conclude that it should be able to handle the load.

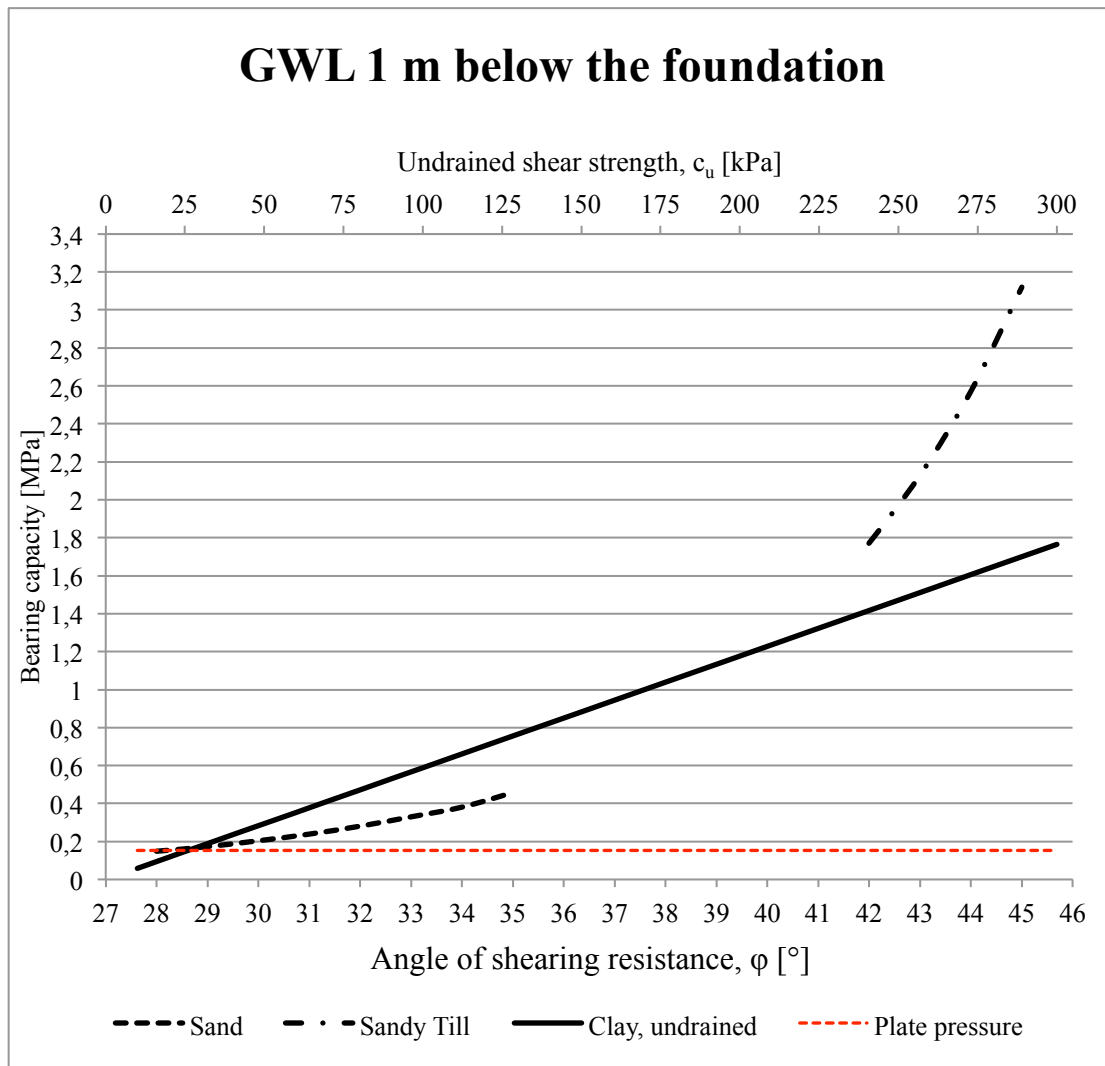


Figure 7.2 Parametric analyses of the bearing capacity for different soil parameters (GWL 1 m below the foundation).

The impact of the GWL is examined in Figure 7.2. The GWL is assumed to be one meter below the foundation, which affects the effective weight of the soil.

The results show that the GWL does not impact the bearing capacity of the clay. This is due to the fact that the bearing capacity of the undrained clay is only dependent on the undrained shear strength  $c_u$ .

In the cases of the sandy till and the sand the GWL has an impact of the bearing capacity. The bearing capacity for sand with an angle of shearing resistance of  $28^\circ$  drops from 222 kPa to 148 kPa when the GWL is one meter under the foundation instead of as previously at great depth. This means that with this GWL the soil's bearing capacity is too low to handle the maximum pressure from the plate. To be able to resist the plate pressure the angle of shearing resistance needs to be at least  $29^\circ$  which corresponds to a bearing capacity of 173 kPa.

For the case of the sandy till the bearing capacity drops with the influence of the ground water but it is still much greater than the plate pressure. For an angle of shearing resistance of  $42^\circ$  the bearing capacity is 1771 kPa.

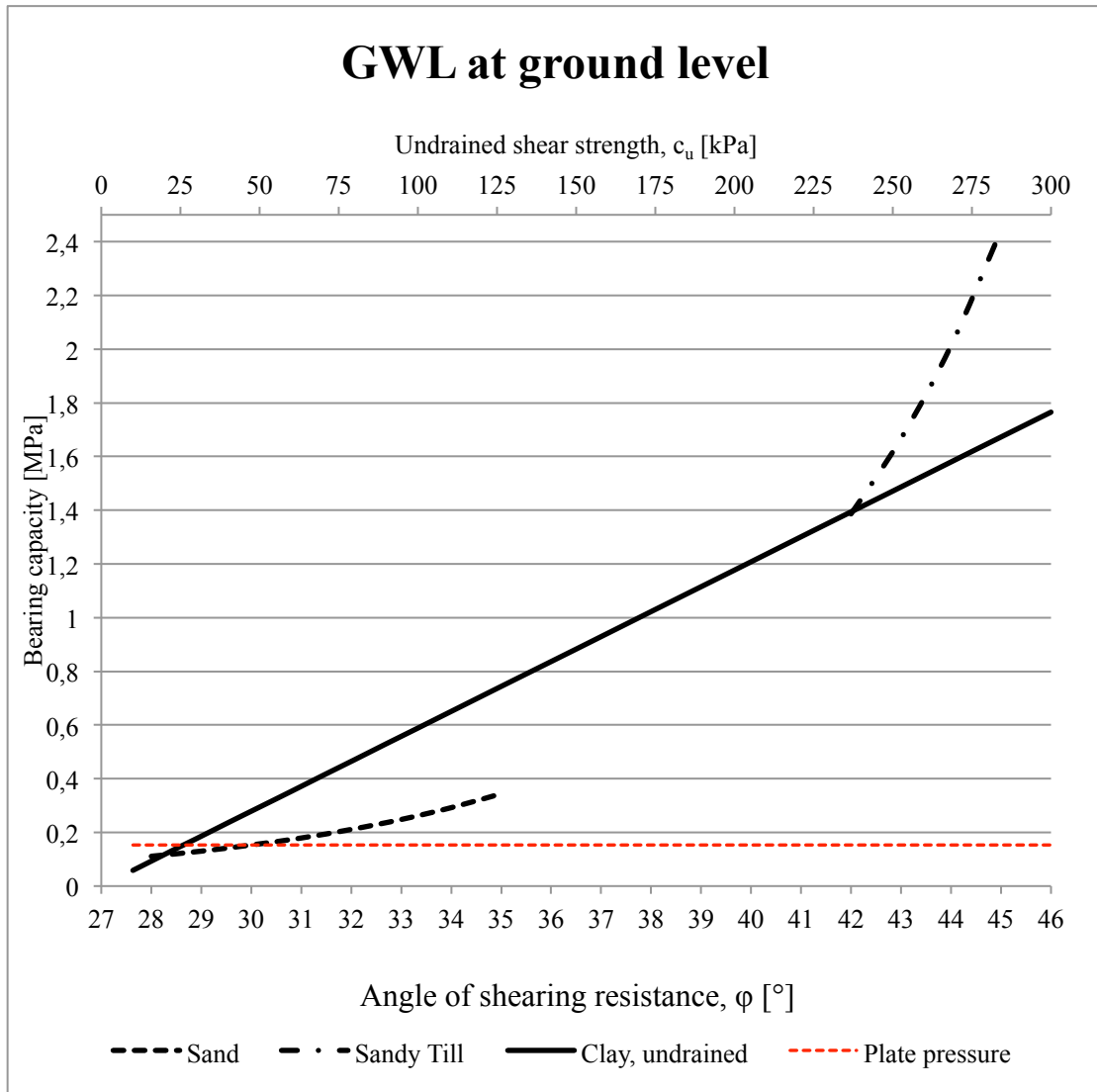


Figure 7.3 Parametric analyses of the bearing capacity for different soil parameters (GWL at ground level).

In the last parametric analysis, GWL is set to the ground level. As mentioned above the groundwater level affects the effective weight of the soil. The effective weight of the soil under GWL is seen in Table 6.1 and the bearing capacity is calculated as in previous cases. In Figure 7.3 the bearing capacity for the different cases are presented.

The bearing capacity for the clay is not affected by the GWL thus the results are the same as in previous cases

To be able to handle the maximum pressure from the plate the sand needs to have at least an angle of shearing resistance of 31°. This angle corresponds to a bearing capacity of 179 kPa, which is relatively close to the plate pressure of 153 kPa.

The result for the case of sandy till shows that with an angle of shearing resistance of 42° the bearing capacity is 1386 kPa. According to the calculations above the bearing capacity for the sandy till should be able to withstand the pressure from plate in every case.

## 7.1.2 PLAXIS 2D

The parametric analyses in PLAXIS 2D only consider the undrained clay and sand case. This is for the reason that sandy till is modelled likewise to sand, but with better strength parameters. Thus the sandy till case is not critical in the analysis.

In this parametric analysis several calculations are made for the two considered cases. For both cases, the same computer models and geometry are used as in previous calculations. The only thing changed is the strength parameters, which are varied in the calculations for all considered position. The load positions in this analysis a centric, edge and corner load on the mat.

Table 7.2 presents the deformation on undrained clay for different values of undrained shear strength,  $c_u$ . The calculations show that the deformation decreases with an increase of shear strength and vice versa. It is also seen that the deflection is greater with a decreased effective area, which the edge and corner calculation proves.

When the load is applied at the centre of the mat, all clay cases in the parametric study are able to handle the pressure. The case with the undrained shear strength of 5 kPa gives a deformation of 56.2 millimetres, which may be too great for the transportation of the wind turbine parts.

Table 7.2 Maximum deflections for clay in PLAXIS 2D

Clay			
$c_u$ [kPa]	Centre [mm]	Edge [mm]	Corner [mm]
5	56.2	*	*
10	28.9	*	*
20	14.7	21.3	*
30	10.4	13.4	101.1
40	8.5	9.7	16.7

\* Numerical failure in the calculation due to the amount of plastic points.

For the cases marked with an asterisk (\*) in Table 7.2 and 7.3, the software refers to a failure of the soil body. The numerical failures occur when the load has developed too many plastic points in the soil, thus the results from these calculations should be treated with caution. The calculations in PLAXIS 2D further prove that the edge and corner load are critical for the mat system.

The parametric analysis for the sand case is with a variation of the angle of shearing resistance. This case also states that the plate will support the given maximum loads for wind turbine transports if the load is applied at the centre. It is more critical at the edges and corners of the mat where plastic deformation will occur.

In Table 7.3 it is seen that all loading positions will handle the load if the angle of shearing resistance is greater than  $32^\circ$ . The deflection increases with a decreased angle of shearing resistance and vice versa.

Table 7.3. Maximum deflection for sand in PLAXIS 2D

Sand			
$\varphi$ [°]	Centre [mm]	Edge [mm]	Corner [mm]
28	11.7	14.0	*
29	11.0	12.6	*
30	10.1	11.5	*
31	9.5	10.6	*
32	9.0	9.9	*
33	8.6	9.3	16.9
34	8.2	8.7	13.4
35	8.0	8.3	10.7

\* Numerical failure in the calculations due to the amount of plastic points.

## 7.2 Comparison of PLAXIS 2D with hand-calculations

The results obtained by the hand-calculations and the calculations in PLAXIS 2D show that there is correlation between the models. However there are some differences that are presented in this chapter.

The greatest deflection obtained from the Winkler model is for the case of clay while the results from PLAXIS 2D show that for some cases the sand has the greatest deflection. The difference between these results can be explained by the values used in the models. The  $k_0$  values for the soils used in the Winkler model are general for that type of soil and are just one value for each soil. It is not specified what type of clay, sand and sandy till that is considered.

In PLAXIS 2D it is possible to use more parameters to explain what type of soil that is under consideration and hence the results are more specific. In PLAXIS 2D the modulus of elasticity and the shear strength determine the deflection of the mat and ground while the subgrade modulus determines the deflection in the Winkler model. Hence to get similar results from the models there should be a correlation between the subgrade modulus  $k_0$  and parameters used in PLAXIS 2D. However for most of the cases the PLAXIS 2D results follow the same pattern as the results for the Winkler model, clay has the greatest deflection while the sandy till has the lowest.

The results show that the amount of deflection differs by approximately a factor of two between the models. The Winkler model only considers the elastic deformation of the soil while PLAXIS 2D also includes the plastic deformation. The difference can explain why the resulting deflection in PLAXIS 2D is twice the amount compared to the deflection obtained in the Winkler model. As mentioned there are some

differences between the models in the case of the deflection, however the shape of the mat is similar in both models.

The results from the general bearing capacity equation and the PLAXIS 2D calculations show that there is a correlation between the models. The bearing capacity for the sand and clay are for both calculations the most critical cases while the bearing capacity for the sandy till is always greater than the pressure from the plate. Both the bearing capacity and the computer calculations give no failures when the angle of shearing resistance is above  $32^\circ$  for the sand case. For the case of clay no failures occur when the undrained shear strength is greater than 30 kPa.

The calculated effective area used in PLAXIS 2D and the general bearing capacity equation differ from each other. The effective area for the corner load has not been taken into account in the hand-calculations due to the assumption that the tire position is 0.5 meters from the centre. However the area for the edge and centre loading in PLAXIS 2D is similar to the effective area used in the bearing capacity calculations.

The results from the two models show that one of the most critical parameter is the effective area. The calculations are based on one detached mat and for that reason the area is limited to 3 times 2.5 meters. Our results have shown that the mat is able to handle the load for all of the cases as long as the load is applied at the centre. This means that the soil is able to bear the pressure from the plate for all of the scenarios studied if the whole plate area spreads the load. Therefore if several mats are connected to each other with connections that have the ability to transfer the pressure, it will increase the effective area of the structure decreasing the pressure transmitted to the soil.

## 8 Discussion

According to the results presented in this thesis it seems that the mat system for most cases is able to handle the load from the transportation. However there are some uncertainties about the mats' behaviour that need to be addressed before claiming that they are suitable for wind turbine transportation.

To be able to perform the calculations for a real case, it is required to investigate the soil properties at site. Shear strength parameters, groundwater level and thickness of the topsoil are all parameters that can be determined by geotechnical investigation. The cases in this study are soil with homogenous layers, which may not reflect how the soil is structured in the field. However, when the soil's strength varies in the soil stratum, averages values for the soil parameters can be used for the calculations, and the results from the parametric analysis show bearing capacity and deformations for a range of values.

The effective area is one of the most sensitive parameters that determine if the mat is able to function as an access road. When applying load close to the edge and corner the effective area supporting the load will be relatively small. For this reason it is necessary to consider a connection system between the mats that has the ability to distribute the load over a larger area. Specific connection systems have not been studied in this thesis, which is a critical part when considering the use of plastic mats as access roads.

The analysis is performed with a maximum load on one dual tire. However, trailers carrying wind turbine components often have several axles to distribute the load. Hence two or three pairs of duals could be on one mat at the same time. The reasons for only analysing one tire load are to investigate critical positions on the mat and due to limitations of the models used. Nevertheless, the effective area distributing the load sets the limit rather than the load itself.

It is also unknown how sensitive the transports are to uneven surfaces. If the lateral gradient of the road is too great there may be a risk for the truck to turn over. This depends on the transport's centre of gravity and the overall balance. The requirement from Vestas is that the lateral gradient should be a maximum of 2 degrees. However, in this thesis only flat surfaces have been considered due to limitations in the models. Whether an inclined or uneven surface affect the bearing capacity or the stability of the transports needs to be investigated.

The maximum allowable deflection is related to the sensitivity of the transports. The sensitivity has not been studied, but to not exceed the requirement of the lateral gradient of 2 degrees the maximum difference in deflection on an axle is calculated to be 70 mm. Therefore if the plastic mats deform equally under an axle, the stability of transport may not be an issue. Nevertheless, the maximum allowable settlement and deflection should be further studied to not risk the safety of the transport nor the road.

## 9 Conclusions

To determine if the mats can be used a proper geotechnical investigation needs to be performed. The parameters that need to be investigated are for non-cohesive soils, sand and sandy till, the angle of shearing resistance and for undrained clay the undrained shear strength. These parameters combined with the groundwater level and the unit weight of the soil can be used to determine the bearing capacity.

According to the results from the hand-calculations and the calculations in PLAXIS 2D the mat is for most cases able to bear the load from the transportation. However, when the effective area is small it may result in failure for some cases of sand and clay. The results indicate that the effective area is the most sensitive parameter if the mat and soil is able to bear the load from the transportation or not. The calculations in this thesis show that as long as the load is distributed over the whole mat the bearing capacity should not be an issue.

The calculations in this thesis are based on one detached mat and how the mat system behaves when connected has not been analysed. However if the connections distribute the load over several mats, the effective area would be even greater than the area analysed in this thesis. Nevertheless even if the mats are connected the calculations for the edge and especially the corner load are valid to show the importance of not driving too near the edges. The results conclude that it is important that the connections between the mats distribute the loads between each other especially if they should be used in soft soils.

The deflection and stress distribution of the mat are highly dependent on the soil condition considered. Clay has as can be seen in the parametric analysis for most cases the greatest deflection while the sandy till has the lowest. With a greater deflection the active area of mat increases, decreasing the stress in the soil. The stress distribution for the special case of soft soil on a dry crust shows that the topsoil deforms while the greatest stress is mobilised in the dry crust. The case shows that it is possible to use the mats as long as the thickness of the top layer is not too great and that the soil beneath has a dry crust with enough strength.

By using temporary plastic mats instead of gravel roads the time and the environmental impact of the construction can be decreased. Groundwork may be necessary to meet the requirements from Vestas, but if a lot of groundwork is needed to improve the soil the positive aspects of using plastic mats will not be that obvious. For that reason there are no calculations made for ground reinforcement in this thesis. Groundwork can increase the stability of the soil but as the results show most cases are able to handle the load from the transports anyway.

## 10 Further studies

Even though the results indicate that the mats can handle the load from the transport it is necessary to do further studies to eliminate the uncertainties mentioned in the discussion. The connection system needs to be studied to see how it distributes the load from one mat to another. A model in 3D with an entire transport should be performed to understand the behaviour of the mat and ground when fully loaded, both static and dynamic. In spite of all calculations and computer software a real field-test is needed to fully understand how the mat and the transport behave on a flexible plastic mat.

## 11 References

- Andersson, P. (2011) *TRVK Väg*. Borlänge: Trafikverket. (TRV 2011:072)
- Andersson, B. (2000) *Kurskompendium Väg-och gatuutformning*. Göteborg: CTH, KTH, LTH.
- Bergdahl, U. Malmberg, B. Ottosson, E. (1993) *Plattgrundläggning*. Solna: AB Svensk Byggtjänst.
- BLM. (2005). *Final Programmatic Environmental Impact Statement on Wind Energy Development on BLM-Administered Lands in the Western United States*. Volume 1. Chapter 3. U.S. Department of the Interior Bureau of Land Management: U.S.A
- Bowles, Joseph E. (1977) *Foundation analysis and design*. New York: McGraw-Hill Book Company.
- Craig, R., Knappett, J. (2012) *Craig's soil mechanics*. 8<sup>th</sup> edition. Oxon: Spon Press.
- Cook, R., Young, W. (1999) *Advanced Mechanics of Materials*. 2<sup>nd</sup> edition. New Jersey: Prentice Hall.
- Gonzalez C., Rushing T. (2010) *Development of new design methodology for structural airfield mats*. International Journal of Pavement Research and Technology Vol.3 No.3: 102-109. May. 2010.
- Hau, E. (2013) *Wind Turbines. Fundamentals, Technologies, Application, Economics*. Berlin Heidelberg: Springer.
- Harry, G. (2010) *Finite Element Analysis of Weight Loading Capabilities of MegaDeck Heavy Duty Matting System on Various Ground Surfaces*. New York 2010
- Huang, Y. (2004) *Pavement Analysis and Design*. 2<sup>nd</sup> edition. New Jersey: Pearson Education.
- Kendrick, P., Copson, M., Beresford S., McCormick P. (2004) *Roadwork-Theory and Practice*. Fifth Edition. Norfolk: Biddles Ltd.
- Larsson, R. (2008) *Jordens egenskaper*. Linköping: SGI (SGI: Information 1)
- Mannering, F., Kilareski, W., Washburn, S. (2005) *Principles of Highway Engineering and Traffic Analysis*. Hoboken, New Jersey: Wiley cop. 2005.
- Maybehire (2007) *Dura-Base Mat-product user guide*. [www.maybehire.co.uk](http://www.maybehire.co.uk) (2014-03-04).
- Megadeckrigmats (2014) *MegaDeck specifications*. [www.megadeckrigmats.com](http://www.megadeckrigmats.com) (2014-03-01).
- Newpark Resources Inc. (2014) *Dura-Base specifications*. [www.newpark.com](http://www.newpark.com) (2014-03-02)
- Nilsson, G. (2003) *Handledning i jordartsklassificering för mindre markvärmesystem*. Linköping: SGI (SGI: Varia 527)
- Nilsson, M. (2010) *Underlagsmaterial för Transporter till vindkraftsparker*. Borlänge: Trafikverket. (2010:032)
- Plaxis (2014) *PLAXIS 2D. Reference Manual* [www.plaxis.nl/plaxis2d/manuals](http://www.plaxis.nl/plaxis2d/manuals) (2014-04-20)

- Robinson, R., Thagesen, B. (2004) *Road engineering for development/ edited by Richard Robinson and Bent Thagesen*. London: Spon Press.
- Subramanian, N. (2010) *Design of Steel Structures*. Oxford: Oxford University Press
- Swedish Standard Institute (SIS). (2008) Eurocode 7 – Geotechnical design – Part 1: General rules, Swedish Edition SS-EN1997-1, Swedish Standards Institute: Stockholm
- Sällfors, G. (2009) *Geoteknik. Jordmateriallära - Jordmekanik*. 4<sup>th</sup> edition. Göteborg: CTH.
- Terzaghi, K. (1967) *Soil Mechanics in Engineering Practice*. 2 ed. New York: Wiley.
- Vestas (2010) *Road, Crane Pad and Hardstand Specifications for Vestas Turbines V100-1.8 MW and V112-3.0MW*. Randers: Vestas. (Vestas report: 0006-4198 V00)
- VTI (2014) Statens väg- och transportforskningsinstitut. [www.vti.se](http://www.vti.se) (2014-03-06)
- Wright, P. Dixon, K. (2004) *Highway Engineering*. Hoboken, New Jersey: Wiley, cop. 2004
- Zigma Ground Solutions (2014) *TuffTrak Specifications*. [www.zigmagroundsolutions.com](http://www.zigmagroundsolutions.com) (2014-03-02)